

INSTITUTE
FOR
COSMIC RAY RESEARCH
UNIVERSITY OF TOKYO

ANNUAL REPORT
(APRIL 2001 – MARCH 2002)

Editorial Board

TAKITA, Masato

KOSHIO, Yusuke

ISSN 0919-8296

©**Institute for Cosmic Ray Research, University of Tokyo**

5-1-5, Kashiwanoha, Kashiwa, Chiba 277-8582 Japan

Phone : (81)4-7136-

3100 (Director),
3101-3114 (Administration Office),
5114 (μ - ν), 5128 (Emulsion),
3176 (Air Shower), 5111 (Kamioka),
5124 (Primary), 5104 (Neutorino Center)

Telex :

Telefax : (81)4-7136-3115

(81)4-7136-3118

Cable :

Printed by
Universal Academy Press, Inc.

Postal Address: C.P.O. Box 235, Tokyo 100-91, JAPAN

Address for Visitors: BR-Hongo-5 Bldg., 6-16-2, Hongo,
Bunkyo-ku, Tokyo 113, JAPAN

Telephone: + 81 3 3813 7232

Facsimile: + 81 3 3813 5932

E-Mail: general@uap.co.jp

WWW URL: <http://www.uap.co.jp>

TABLE OF CONTENTS

Preface	1
Research Divisions	1
Kamioka	
μ - ν (+ Primary Cosmic Ray)	
Air Shower	
Emulsion	
Neutrino Center	
Observatories and Stations	33
Norikura Observatory	
Akeno Observatory	
Appendix A. ICRR International Workshop	41
Appendix B. Seminar in 2001	42
Appendix C. List of Publications	43
(a) Papers Published in Journals	
(b) Conference Papers	
(c) ICRR-Report	
Appendix D. Doctoral Theses	46
Appendix E. Public Relations	46
ICRR News	
Appendix F. List of Committee Members	47
(a) Board of Councillors	
(b) Executive Committee	
(c) Advisory Committee	
Appendix G. List of Personnel	48

PREFACE

It is a pleasure to bring to you our annual report for the fiscal year 2001, describing various activities of Institute for Cosmic Ray Research (ICRR), the University of Tokyo.

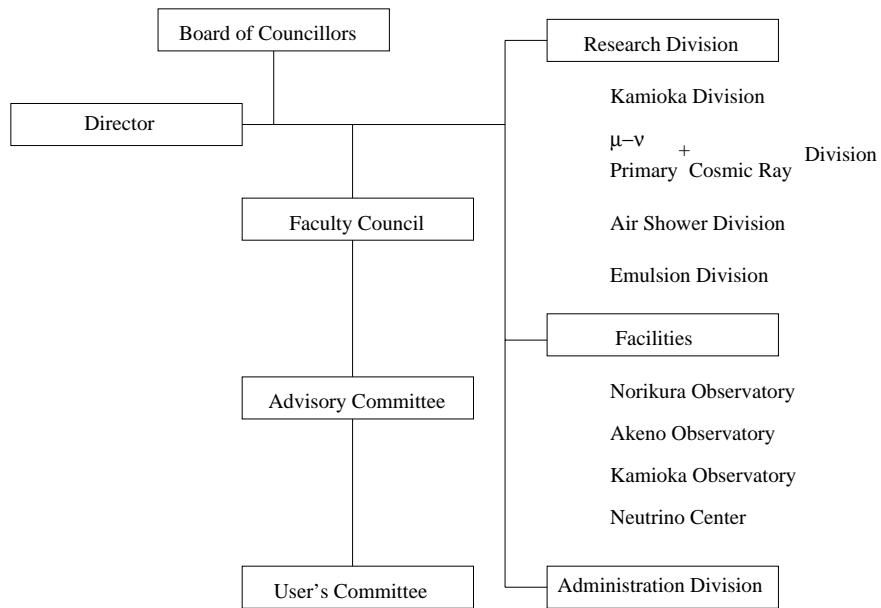
ICRR is an institute closely associated with Japanese universities. ICRR thus hosts or co-hosts several experimental facilities which are jointly used by about 350 researchers and graduate students of universities. Major experiments done in collaboration are Super-Kamiokande at Kamioka Observatory, AGASA at Akeno Observatory, CANGAROO at Woomera in Australia, Tibet-AS-Gamma in Tibet, and TAMA 300 at National Astronomical Observatory. These experiments are quite unique compared with other competing experiments in the world and some of them have already produced very important results which are described in this volume.

Cosmic ray physics today presents major challenges to probe physics beyond the standard theory of the micro-world: discovery and refinement of neutrino oscillation via the atmospheric neutrino observation is the most important step towards further unification beyond what we firmly established in the standard model. Besides the neutrino beam which nature gave us fortuitously there now exists the man-made beam directed to Super-K from KEK at Tsukuba. An intermediate result of this K2K experiment so far presented is compatible with result obtained from the atmospheric neutrino oscillation at Super-K. In another frontier TeV gamma rays observed by CANGAROO shed new light on the origin of high energy cosmic ray. Despite of the firm confidence that underlines the existence of the GZK cutoff highest energy cosmic rays beyond this cutoff are kept observed by AGASA. This is perhaps a subject to be examined in more detail by the next generation of detectors such as AUGER and Telescope Array.

We hope to continue to make major contribution to cosmic ray physics in the world in coming years.

Motohiko Yoshimura, Director of ICRR

Organization



Number of Staff Members in 2001

	Scientific Staff	Technical Staff	Research Fellows	Administrators and Secretaries	
Director	1				
Kamioka	10		2	3	
μ - ν + Primary	5	2	3		
Air Shower	9	4	5	1	
Emulsion	4	2	10		
Neutrino Center	3	1	1	1	
Guest	4				
Norikura		3			
Administration				7	
Total	36	12	21	12	81

FY 1996–2001 Budget

	1996	1997	1998	1999	2000	2001
Personnel expenses	476 072	572 318	536 510	569 050	589 879	418 475
Non-personnel expenses	1 259 435	1 278 788	1 680 983	1 411 063	1 423 789	1 518 584
Total	1 735 507	1 851 106	2 217 493	1 980 113	2 013 668	1 937 059

(in 1 000 yen)

KAMIOKA DIVISION

Super-Kamiokande

Overview

Super-Kamiokande (SK) is a large water Cherenkov detector, located 1000 m underground in Kamioka mine, Japan. 50 kton of pure water is contained in a stainless steel tank of 39.3 meters in diameter and 41.4 m in height. The main purpose of the SK detector is the detection of atmospheric neutrinos, solar neutrinos, supernova neutrinos, and search for nucleon decays. SK had been taking data from April 1996 to July 2001 using 11,146 20-inch photomultipliers (PMTs) for inner detector and 1,885 8-inch PMTs for outer detector. In 2001, several hundred bad PMTs were replaced. While filling pure water into the SK tank after the PMT replacement, large number of PMTs were destroyed on November 12, 2001. The detector was reconstructed in 2002 using about 5200 20-inch PMTs. Pure water was filled from October to December in 2002 and data taking with full water was started from December 2002.

During the first five years of data taking, SK has established neutrino oscillations in atmospheric neutrinos and solar neutrinos. Furthermore, the long baseline accelerator neutrino experiment (K2K), which has been running since 1999, confirmed the ν_μ oscillations.

In this report, those results obtained by SK and K2K are described.

Atmospheric neutrinos

Cosmic ray interactions in the atmosphere produce neutrinos. The prediction of the absolute flux has an uncertainty of at least $\pm 20\%$. However, the flavor ratio of the atmospheric neutrino flux, $(\nu_\mu + \bar{\nu}_\mu)/(\nu_e + \bar{\nu}_e)$, has been calculated to an accuracy of better than 5% in a broad energy range from 0.1 GeV to higher than 10 GeV. The fluxes of upward and downward going neutrinos are expected to be nearly equal for $E_\nu >$ (a few GeV).

SK observed 11,872 fully-contained (FC) events and 913 partially-contained (PC) events during 1489 days of data taking. FC events deposit all of their Cherenkov light in the inner detector, while PC events have exiting tracks which deposit some Cherenkov light in the outer detector. The neutrino interaction vertex was required to have been reconstructed within the 22.5 kiloton fiducial volume, defined to be > 2 m from the PMT wall.

The FC events were classified into “sub-GeV” ($E_{vis} < 1330$ MeV) and “multi-GeV” ($E_{vis} > 1330$ MeV) samples. The numbers of observed and predicted events for sub- and multi-GeV energy regions in SK are summarized in Table 1. Among FC events, single-ring events are identified as e -like or μ -like based on a Cherenkov ring pattern. All the PC events were assigned to be multi-GeV μ -like. Using the number of e -like and μ -like events, the ratio of (μ/e) was obtained and it is significantly smaller

Table 1. Summary of the atmospheric $(\mu/e)_{data}/(\mu/e)_{MC}$ ($\equiv R$) ratio measurement.

	Data	MC
Sub-GeV		
e -like	3266	3081.0
μ -like	3181	4703.9
$R = 0.638 \pm 0.016 \pm 0.050$		
Multi-GeV		
e -like	772	707.8
μ -like(FC+PC)	1577	2198.2
$R = 0.658^{+0.030}_{-0.028} \pm 0.078$		

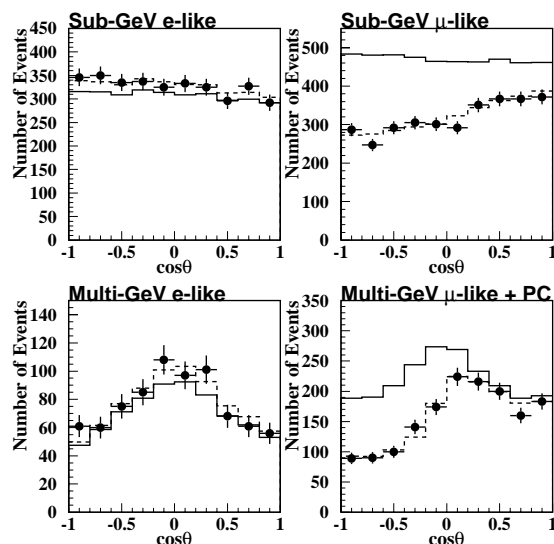


Fig. 1. Zenith angle distributions for sub-GeV e -like, sub-GeV μ -like, multi-GeV e -like and multi-GeV (FC+PC) μ -like events. $\cos \Theta = 1$ means down-going particles. The solid histograms show the MC prediction for the no neutrino oscillation case. The dotted histograms show the Monte Carlo prediction for $\nu_\mu \leftrightarrow \nu_\tau$ oscillations with $\sin^2 2\theta = 1$ and $\Delta m^2 = 2.5 \times 10^{-3} \text{ eV}^2$.

than the expectation as shown in the table.

The zenith angle distributions for the sub- and multi-GeV samples are shown in Fig. 1. The μ -like data from SK exhibited a strong up-down asymmetry in zenith angle (Θ) while no significant asymmetry was observed in the e -like data. The data were compared with the Monte Carlo expectation without neutrino oscillations and the best-fit expectation for $\nu_\mu \leftrightarrow \nu_\tau$ oscillations. The oscillated Monte Carlo well reproduced the zenith angle distributions of the data. Some fraction of the multi-ring event are also subdivided into e -like and μ -like events using the event pattern of the most energetic Cherenkov ring in each event. Figure 2 shows the zenith angle distribution of multi-ring events and they also agree well with the expectations from neutrino oscillations.

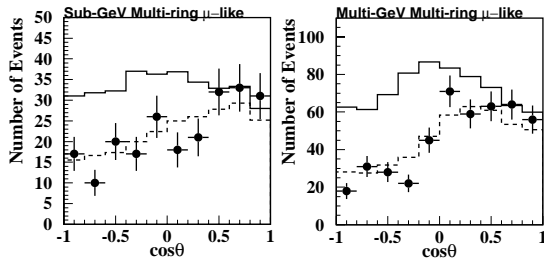


Fig. 2. Zenith angle distributions for multi-ring sub-GeV μ -like (left) and multi-ring multi-GeV μ -like samples. The solid and dashed histograms show expectations without and with neutrino oscillations, respectively.

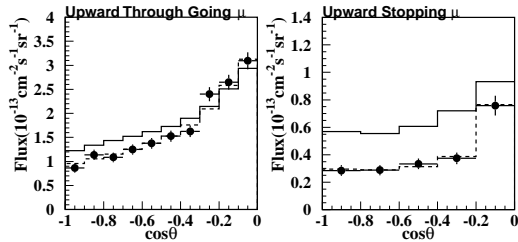


Fig. 3. Zenith angle distributions of upward through-going muons (left) and upward stopping muons (right). The solid histogram shows the expected flux for the null neutrino oscillation case. The dashed histogram shows the expected flux for the $\nu_\mu \leftrightarrow \nu_\tau$ oscillation with $\sin^2 2\theta = 1.0$ and $\Delta m^2 = 2.5 \times 10^{-3} \text{ eV}^2$.

Energetic atmospheric ν_μ 's passing through the Earth interact with rock surrounding the detector and produce muons via charged current interactions. These neutrino events are observed as upward going muons. Upward going muons are classified into two types. One is “upward through-going muons” which have passed through the detector, and the other is “upward stopping muons” which come into the detector and stop inside the detector. The mean neutrino energy of upward through-going muons and upward stopping muons are $\sim 100 \text{ GeV}$ and $\sim 10 \text{ GeV}$, respectively. SK has observed 1878 upward through-going muons and 456 upward stopping muons during 1678 and 1657 days' live time, respectively. Fig. 3 shows the zenith-angle distributions of those upward muons. They agree with the expectations with neutrino oscillations.

We carried out a neutrino oscillation analysis using all the SK atmospheric neutrino data. Fig. 4 shows the allowed neutrino oscillation parameter region for $\nu_\mu \leftrightarrow \nu_\tau$ oscillations obtained by this analysis. The best fit oscillation parameters are $\sin^2 2\theta = 1.0$ and $\Delta m^2 = 2.5 \times 10^{-3} \text{ eV}^2$. The allowed oscillation parameter range is obtained to be $\sin^2 2\theta > 0.92$ and $\Delta m^2 = (1.6 - 3.9) \times 10^{-3} \text{ eV}^2$ at 90% C.L.

The neutrino oscillation analysis described above assumed $\nu_\mu \leftrightarrow \nu_\tau$ oscillations. The possibility of $\nu_\mu \leftrightarrow \nu_s$ (sterile neutrinos) oscillation was investigated using two methods, one using the MSW effect for oscillations and another using a neutral current (NC) enriched sample. The forward scattering amplitude of ν_μ and ν_τ are same, but that of ν_s is different. The difference in the ampli-

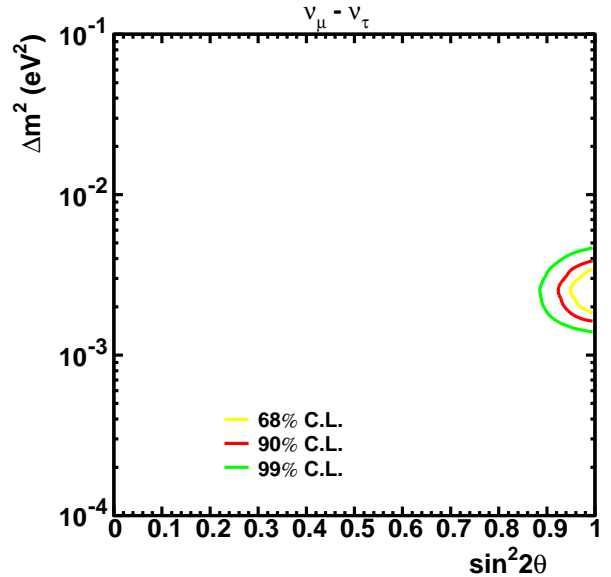


Fig. 4. Allowed region of $\nu_\mu \rightarrow \nu_\tau$ neutrino oscillation parameters obtained by SK by using contained atmospheric neutrino events and the upward-going muon events.

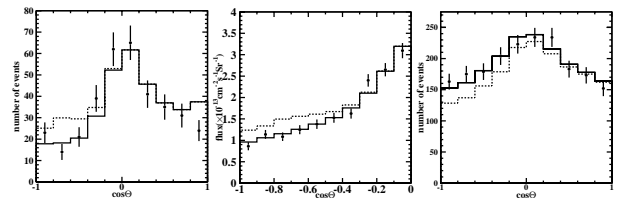


Fig. 5. Zenith angle distribution of higher energy PC events (left), upward-going muons (middle) and NC enriched sample (right). The solid and dashed histograms show expectations for $\nu_\mu \leftrightarrow \nu_\tau$ and $\nu_\mu \leftrightarrow \nu_s$ oscillations, respectively, assuming $\Delta m^2 = 3 \times 10^{-3} \text{ eV}^2$ and $\sin^2 2\theta = 1$.

tude causes suppression of neutrino oscillations for higher energy neutrinos. Figure 5 (left) shows zenith angle distribution of high energy PC events ($E > 5 \text{ GeV}$, $\langle E \rangle = \sim 25 \text{ GeV}$) together with expected distributions for $\nu_\mu \leftrightarrow \nu_\tau$ and $\nu_\mu \leftrightarrow \nu_s$ oscillations assuming $\Delta m^2 = 3 \times 10^{-3} \text{ eV}^2$ and $\sin^2 2\theta = 1$.

The same figure for upward-through-going muons is shown in Fig. 5 (middle). The second method to discriminate $\nu_\mu \leftrightarrow \nu_\tau$ and $\nu_\mu \leftrightarrow \nu_s$ oscillations is using NC events. In case of $\nu_\mu \leftrightarrow \nu_\tau$ oscillations, the event rate of NC interaction should be same as null oscillations. On the other hand, the NC event rate is smaller for $\nu_\mu \leftrightarrow \nu_s$. A NC enriched sample was made requiring multi-ring event pattern and the most energetic ring to be e-like. The estimated fraction of NC event is 29% in the sample. The observed zenith angle distribution of the sample is shown in Fig. 5 (right). Those distributions show that the pure $\nu_\mu \leftrightarrow \nu_\tau$ hypothesis fits better than the pure $\nu_\mu \leftrightarrow \nu_s$ hypothesis. Scanning all possible Δm^2 and $\sin^2 2\theta$ ranges, pure $\nu_\mu \leftrightarrow \nu_s$ oscillations are disfavored with more than 99% C.L.

We have also performed a search for the appearance of

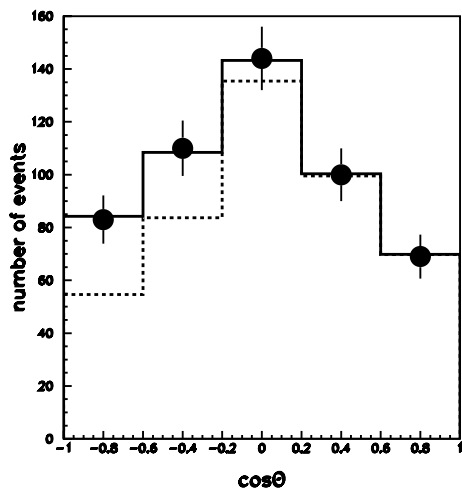


Fig. 6. Zenith angle distribution of τ -like events. The solid and dashed histograms show expectations with and without τ appearance.

ν_τ events. The charged current interaction of ν_τ produces τ . The signatures of τ -decays are (1) larger multiplicity of Cherenkov rings, (2) larger number of decay electrons, and (3) relatively spherical event pattern, and so on. A likelihood of τ -like events are made based on those signatures. Fig. 6 shows zenith angle distribution of the events which give larger τ likelihood. Excess of events above the expectations without τ indicates the appearance of τ events. The excess number of τ -like events is 145 ± 44 (stat.) $_{-16}^{+11}$ (sys.). It is consistent with the expectation of 86 events for the oscillation parameters obtained above.

Solar neutrinos

The observed flux by the solar neutrino experiments (Homestake, Kamiokande, Super-Kamiokande, Gallium experiments, and SNO charged current) were lower than the expectations from the Standard Solar Model (SSM), which has been known as “solar neutrino problem”. The precise measurement of solar neutrinos by SK and SNO established that the solar neutrino problem is due to neutrino oscillations.

SK detects ^8B solar neutrinos through neutrino-electron scattering, $\nu + e \rightarrow \nu + e$. The electron energy, direction and the time of the events are measured. The $\nu + e \rightarrow \nu + e$ method of the solar neutrino detection is sensitive not only to ν_e but also to ν_μ and ν_τ . The cross section of $\nu_\mu + e$ and $\nu_\tau + e$ scatterings are about $\frac{1}{7}$ of that of $\nu_e + e$.

In order to perform precise solar neutrino measurement, the energy scale, the energy resolution, the angular resolution and the vertex position resolution were precisely calibrated using LINAC system and ^{16}N events generated by a DT neutron generator. The absolute energy scale was calibrated with an accuracy of $\sim 0.6\%$.

Figure 7 shows the angular distribution to the direction of the sun. SK has observed about 22,000 solar neutrino events above 5 MeV during 1496 days of live

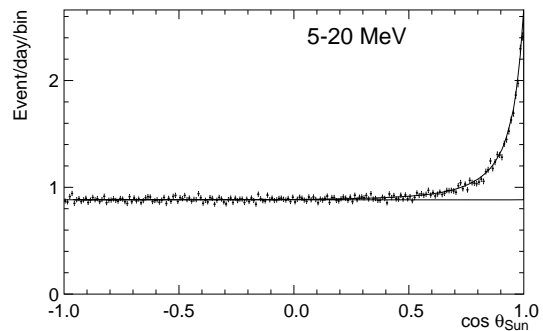


Fig. 7. Angular distribution to the direction of the sun.

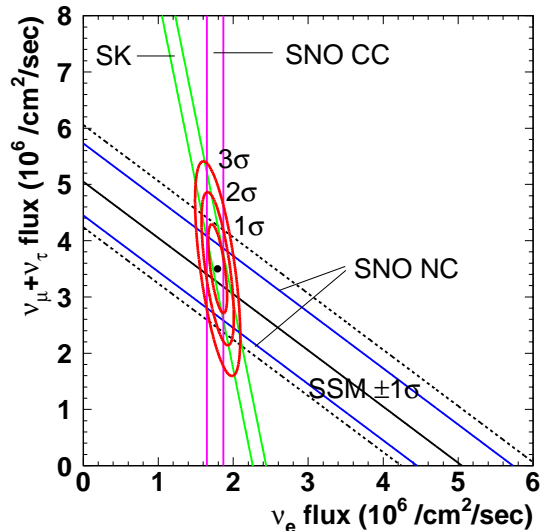


Fig. 8. ν_e flux and $\nu_\mu + \nu_\tau$ flux contour obtained by SK and SNO data.

time. This number corresponds to the ^8B solar ν flux of 2.35 ± 0.02 (stat.) ± 0.08 (sys.) $\times 10^6 \text{ cm}^{-2} \text{ s}^{-1}$, which is 46.5 ± 0.5 (stat.) $_{-1.5}^{+1.6}$ (sys.)% of the SSM prediction. Recently, Sudbury Neutrino Observatory (SNO) presented their results of the charged current (CC), neutral current (NC), and electron scattering (ES) fluxes. SNO is a Cherenkov detector using 1000 ton heavy water. Their CC flux, to which only ν_e contributes, was $1.76_{-0.05}^{+0.06}$ (stat.) ± 0.09 (sys.) $\times 10^6 \text{ cm}^{-2} \text{ s}^{-1}$. The 4.2σ higher flux in SK shows the existence of the ν_μ and/or ν_τ in solar neutrinos observed at earth. It is the direct evidence for solar neutrino oscillations. Figure 7 shows flux of ν_e and $\nu_\mu + \nu_\tau$ obtained by SK flux, SNO CC flux and SNO NC flux. The total neutrino flux obtained by those measurement is consistent with the SSM prediction as shown in the figure.

Combining the flux measurements by SK, SNO, Homestake, and gallium experiments, several allowed regions (flux global solutions) remain as shown in Fig. 8. The precise measurement of energy spectrum and day/night variation by SK enable us to discuss the oscillation parameters. Figure 9 shows the recoil electron spectrum normalized by SSM prediction. Expectations from each flux global solutions are shown in the figure. The Small Mixing Angle (SMA) and just-so solutions expect distortion of the energy spectrum. However, the SK energy

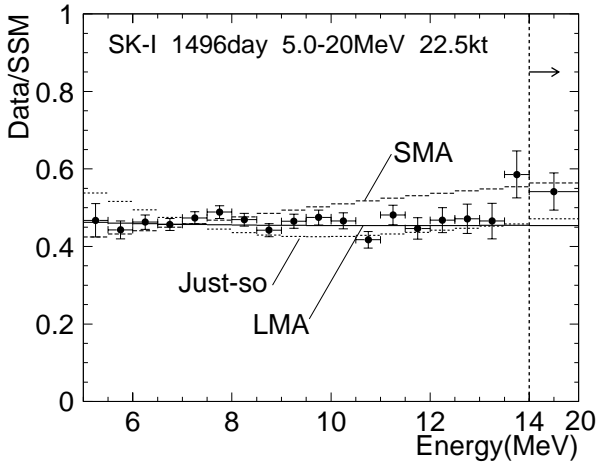


Fig. 9. Recoil electron energy spectrum of solar neutrinos. Ratio of the observed spectrum to the expected spectrum is shown. The solid, dashed and dotted histograms show typical large mixing angle (LMA), small mixing angle (SMA), and just-so solutions. $\nu_e \leftrightarrow \nu_\mu(\nu_\tau)$ oscillations are assumed.

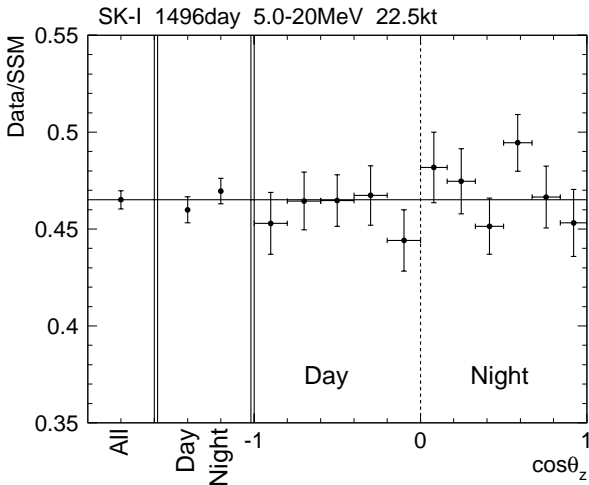


Fig. 10. Day/night variation data. The day and night time data are sub-divided as a function of the zenith angle of the sun.

spectrum is nearly flat. Figure 10 shows the day/night variation. The day/night difference is expressed as:

$$\frac{Night - Day}{\frac{1}{2}(Day + Night)} = 0.021 \pm 0.020^{+0.013}_{-0.012}.$$

The measured energy spectrum and day/night difference are used to constrain neutrino oscillation parameters. The energy range of the solar neutrino spectrum is divided into 8 energy bins and day/night is divided into one bin for day and 6 bins for night according to the zenith angle of the sun. Fig. 11 shows the excluded region by the SK zenith-spectrum analysis overlaid with the allowed regions obtained by the flux global analysis. SMA, just-so, and LOW solutions are disfavored with more than 95% C.L. The absolute flux is a free parameter in this analysis. By constraining the total flux of ^8B neutrinos either using the SSM prediction or SNO NC

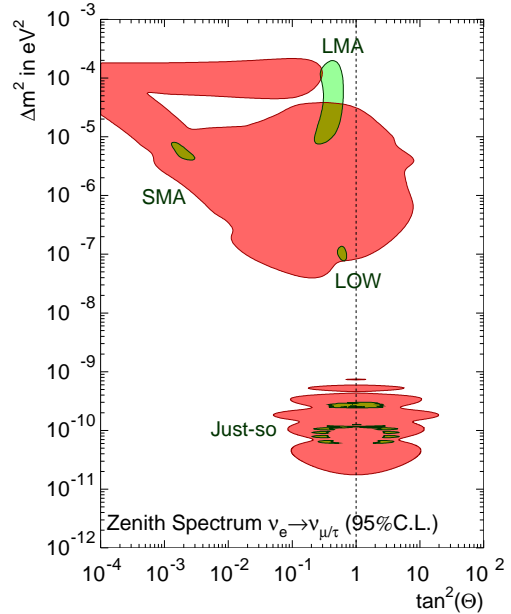


Fig. 11. Exclusion area for $\nu_e \leftrightarrow \nu_\mu/\nu_\tau$ from (flux-independent) zenith-spectrum analysis at 95% confidence level. The separate regions with the names are allowed regions based on the absolute fluxes measured by solar neutrino experiments.

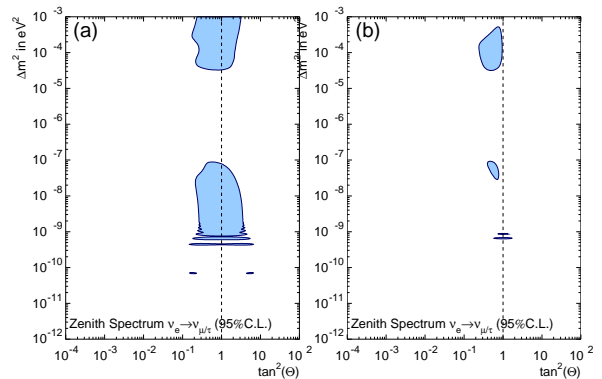


Fig. 12. Allowed regions of neutrino oscillation parameters from SK zenith spectrum. The flux is constrained by (a) the SSM prediction and (b) SNO CC and NC flux measurements.

and CC flux measurements, allowed regions of oscillation parameters are obtained using SK zenith-spectrum as shown in Fig. 12. Only large mixing angle solutions are allowed.

Combining the results of SK measurement, SNO flux measurements, and radiochemical experiments (Homesake, GALLEX and SAGE), a single allowed region of oscillation parameters is obtained as shown in Fig. 13. The confidence level of other solutions are less than 2%. The obtained solution is only LMA solution and it is the sensitive region of KamLAND experiment.

Search for nucleon decay

One of the most unique predictions of Grand Unified Theories (GUTs) is baryon number violation. In many

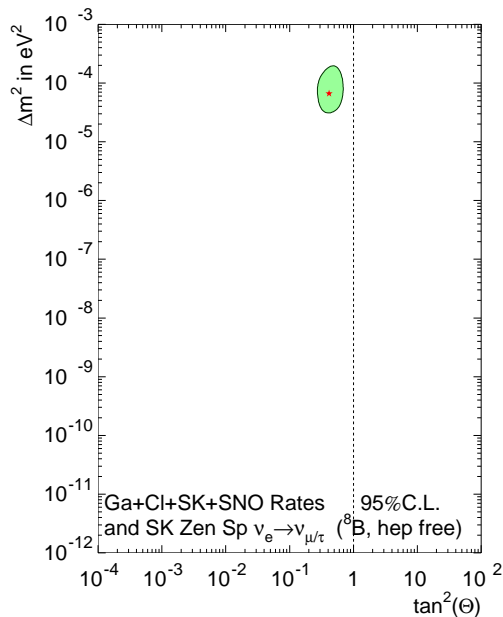


Fig. 13. Allowed region obtained by combining SK zenith spectrum, SNO CC and NC measurements, and radiochemical experiments.

GUT models, either $p \rightarrow e^+\pi^0$ or $p \rightarrow \bar{\nu}K^+$ is the dominant decay modes.

$p \rightarrow e^+\pi^0$: This decay mode has a characteristic event signature, in which the electromagnetic shower caused by the positron is balanced against the two showers caused by the gamma rays from the decay of the π^0 .

We searched for proton decay events in the fully-contained atmospheric neutrino sample. The essential selection criteria are: $800 < \text{total invariant mass} < 1050 \text{ MeV}/c^2$ and total momentum $< 250 \text{ MeV}/c$ in addition to requirements on the number of rings, particle type, π^0 mass and $\mu \rightarrow e$ decay. The detection efficiency is estimated to be 40%. The expected number of background events was 0.3. No candidate event was observed. The lower limit on the partial lifetime for $p \rightarrow e^+\pi^0$ was obtained to be $\tau/B_{p \rightarrow e^+\pi^0} > 5.4 \times 10^{33}$ years at 90% C.L.

$p \rightarrow \bar{\nu}K^+$: The momentum of the K^+ from $p \rightarrow \bar{\nu}K^+$ is $340 \text{ MeV}/c$ and is below the threshold momentum for producing Cherenkov light in water. Candidate events for this decay mode are therefore identified through the decay products of the K^+ : $K^+ \rightarrow \mu^+\nu$ and $K^+ \rightarrow \pi^+\pi^0$.

Two separate decay methods were used to search for $K^+ \rightarrow \mu^+\nu$. The first method searched for the mono-energetic muons from the stopped K^+ . The signal can be found as an excess of single-ring μ -like events at $236 \text{ MeV}/c$ above the continuous background due to atmospheric neutrino interactions. In the second method, a coincidence of a γ (from $^{16}\text{N}^*$ and a delayed μ (from K^+) was required.

By combining all the three results, no evidence for $p \rightarrow \bar{\nu}K^+$ was observed and the lower limit of the partial lifetime for this mode was obtained to be 2.2×10^{33} yr

at 90% C.L.

Analyses of other nucleon decay modes and the improvements of the analysis in for these two modes are in progress.

List of Publications

The number of citations before January 2003 is shown.

- [1] Fukuda, Y. et al. 1998, Measurement of a small atmospheric ν_μ/ν_e ratio, *Phys. Lett. B*, 433, 9–18.
The number of citations: 534
- [2] Fukuda, Y. et al. 1998a, Study of the atmospheric neutrino flux in the multi-GeV energy range, *Phys. Lett. B*, 436, 33–41.
The number of citations: 525
- [3] Fukuda, Y. et al. 1998b, Measurements of the solar neutrino flux from Super-Kamiokande's first 300 days, *Phys. Rev. Lett.*, 81, 1158–1162.
The number of citations: 385
- [4] Shiozawa, M. et al. 1998, Search for proton decay via $p \rightarrow e^+\pi^0$ in a large water Cherenkov detector, *Phys. Rev. Lett.*, 81, 3319–3323.
The number of citations: 54
- [5] Fukuda, Y. et al. 1998c, Evidence for oscillation of atmospheric neutrinos, *Phys. Rev. Lett.*, 81, 1562–1567.
The number of citations: 1599
- [6] Nakahata, M. et al. 1999, Calibration of Super-Kamiokande using an electron LINAC, *Nucl. Inst. Meth. A*, 421, 113–129.
The number of citations: 40
- [7] Fukuda, Y. et al. 1999, Constraints on neutrino oscillation parameters from the measurement of day-night solar neutrino fluxes at Super-Kamiokande, *Phys. Rev. Lett.*, 82, 1810–1814.
The number of citations: 293
- [8] Fukuda, Y. et al. 1999a, Measurements of the solar neutrino energy spectrum using neutrino-electron scattering, *Phys. Rev. Lett.*, 82, 2430–2434.
The number of citations: 274
- [9] Fukuda, Y. et al. 1999b, Measurements of the flux and zenith-angle distribution of upward through-going muons by Super-Kamiokande, *Phys. Rev. Lett.*, 82, 2644–2648.
The number of citations: 379
- [10] Fukuda, Y. et al. 1999c, Neutrino induced upward stopping muons in Super-Kamiokande *Phys. Lett.*, B467, 185–193.
The number of citations: 138
- [11] Futagami, T. et al. 1999, Observation of the east-west anisotropy of the atmospheric neutrino flux, *Phys. Rev. Lett.*, 82, 5194–5197.
The number of citations: 49

- [12] Takeuchi, Y. et al. 1999, Measurements of Radon concentrations at Super-Kamiokande, *Phys. Lett. B*, 452, 418–424.

The number of citations: 4

- [13] Hayato, Y. et al. 1999, Search for proton decay through $p \rightarrow \bar{\nu}K^+$ in a large water Cherenkov detector, *Phys. Rev. Lett.*, 83, 1529–1533.

The number of citations: 46

- [14] Blaufuss, E. et al. 2001, N-16 as a calibration source for Super-Kamiokande, *Nucl. Inst. Meth. A*, 458, 638–649.

The number of citations: 2

- [15] Fukuda, S. et al. 2000, Tau neutrinos favored over sterile neutrinos in atmospheric muon-neutrino oscillations. *Phys. Rev. Lett.*, 85, 3999–4003.

The number of citations: 330

- [16] Fukuda, S. et al. 2001, Solar B-8 and hep neutrino measurements from 1258 days of Super-Kamiokande data. *Phys. Rev. Lett.*, 86, 5651–5655.

The number of citations: 340

- [17] Fukuda, S. et al. 2001a, Constraints on neutrino oscillations using 1258 days of Super-Kamiokande solar neutrino data. *Phys. Rev. Lett.*, 86, 5656–5660.

The number of citations: 282

- [18] Fukuda, S. et al. 2002, Search for neutrinos from gamma-ray bursts using Super-Kamiokande. *Ap. J.*, 578.

- [19] Fukuda, S. et al. 2002a, Determination of solar neutrino oscillation parameters using 1496 days of Super-Kamiokande data. *Phys. Lett. B*, 539, 179–187.

The number of citations: 70

Collaboration

Institute	Country	(*)
ICRR, Univ. of Tokyo	Japan	22
Boston Univ.	USA	7
BNL	USA	1
Univ. of California, Irvine	USA	9
California State Univ.	USA	3
George Mason Univ.	USA	1
Gifu Univ.	Japan	1
Univ. of Hawaii	USA	4
KEK	Japan	9
Kobe Univ.	Japan	2
kyoto Univ.	Japan	5
LANL	USA	1
Louisiana State Univ.	USA	3
Univ. of Maryland	USA	6
MIT	USA	1
Univ. of Minnesota	USA	1
State Univ. of New York, Stony Brook	USA	10
Niigata Univ.	Japan	4
Osaka Univ.	Japan	3
Seoul National Univ.	Korea	3
Shizuoka Seika College	Japan	1
Tohoku Univ.	Japan	7
Univ. of Tokyo	Japan	1
Tokai Univ.	Japan	4
Tokyo Institute of Technology	Japan	4
Warsaw Univ.	Poland	1
Univ. of Washington	USA	4

(*) Number of participants.

K2K

Overview

The first long baseline neutrino oscillation experiment was conducted. The neutrino beam produced at the KEK-PS was directed to the Super-Kamiokande detector, 250 km away from the neutrino production target. The experiment is sensitive to the neutrino oscillation for $\Delta m^2 \geq 3 \times 10^{-3} \text{ eV}^2$ with large mixing angles. The observation of the atmospheric neutrino oscillation by Super-Kamiokande will be tested experimentally and the precise oscillation parameters would be determined. About 4.8×10^{19} protons on target were used to produce neutrinos from April 1999 to July 2001. A total of 56 neutrinos from KEK have been identified in the Super-Kamiokande detector, while the expected number of events in the absence of neutrino oscillation was $80.1_{-5.4}^{+6.2}$. Distortion of neutrino energy spectrum reconstructed from 29 fully-contained single ring events was also observed. Thus, the probability that the observed flux at Super-Kamiokande is explained by statistical fluctuation without neutrino oscillations is less than 1%. Allowed region of Δm^2 at 90% C.L. is $1.5 \sim 3.9 \times 10^{-3} \text{ eV}^2$ at the maximal mixing. K2K experiment has resumed its data taking since Dec, 2003 and will continue until early 2005. By that time, the number of neutrino events should be twice larger than at present.

The Long Baseline Neutrino Oscillation Experiment

The discovery of the neutrino oscillation by Super-Kamiokande in 1998, has lead to the conclusion that neutrino has a finite mass. The discovery implies the existence of new

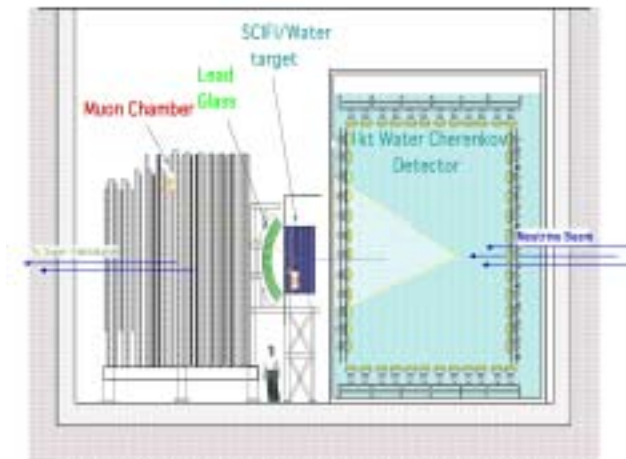


Fig. 14. The arrangement of the near detectors.

physics beyond the standard model of the elementary particles with a huge energy scale. Since the observed neutrino mass difference of $\Delta m^2 \sim 3 \times 10^{-3} \text{eV}^2$ suggests the oscillation length is about a few hundred km for one GeV neutrinos, this observation can be experimentally tested by using the artificially created neutrino beam with the detector placed at a few hundred km from the neutrino production point.

The k2k experiment was planned to detect such oscillation effect and to determine the oscillation parameters precisely. The neutrino beam created at KEK has a mean energy of 1.3 GeV and was sent to the Super-Kamiokande detector, 250 km west of KEK, every 2.2 seconds with the duration of $1.1 \mu\text{sec}$. In the site of KEK, at the distance of 300 m from the target, we have prepared near detectors which mainly consist of 1kt water Cherenkov detector, fine grained scintillation fiber detector (FGD) and the muon ranger. The supplemental detectors are also placed. The arrangement of the front detectors is shown in Fig. 14.

There are several beam monitors, proton profile monitors, the muon monitor and the pion monitor, placed along the neutrino beam line. The decay length is about 200 m, therefore the beam is not scaled exactly by $1/r^2$ law. The flux ratio of the near to the far detector was obtained by the beam Monte Carlo calculation by taking account of the spread and emittance of the beam at the target, the production of the pions, the focusing effect by the HORN and the decay of pions to neutrinos. The beam calculation was validated by the pion monitor which measured the produced pion directions and momentum.

The beam flux and the spectrum were measured by the front detectors. ICRR group has a responsibility of providing the Super-Kamiokande data and the construction of the 1kt front detector and the analysis of the data from those detector components. The coverage of PMT in the 1kt front detector is same as the Super-Kamiokande detector with the 40% of the total inner detector surface. The 1kt detector provides information of the absolute neutrino flux and the spectrum of the neutrino beam. Figure 15 shows the muon momentum spectrum obtained by using the single ring fully contained events at 1kt detector. The observed spectrum is well reproduced by the Monte Carlo simulation in which beam energy spectrum and neutrino interaction in water are taken into account. Combining the 1kt data and FGD data together with constraint of the pion monitor measurement, the expected

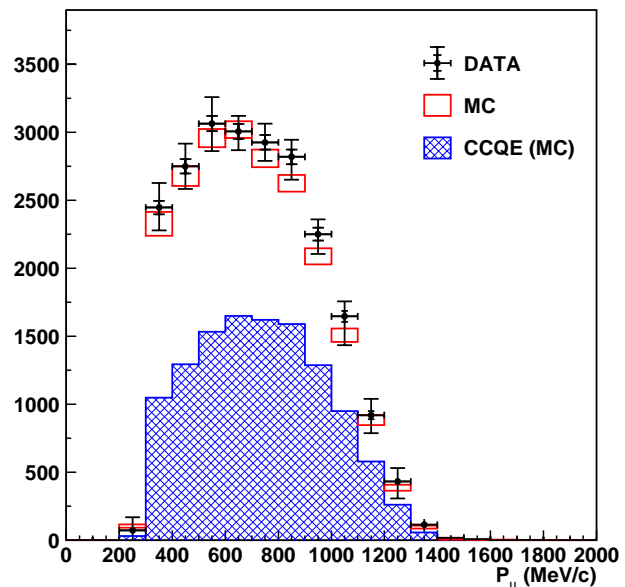


Fig. 15. The muon momentum spectrum obtained by using single ring fully contained events at the 1kt detector. The box shows the corresponding Monte Carlo simulation. The hatched histogram shows CC quasi-elastic component in MC.

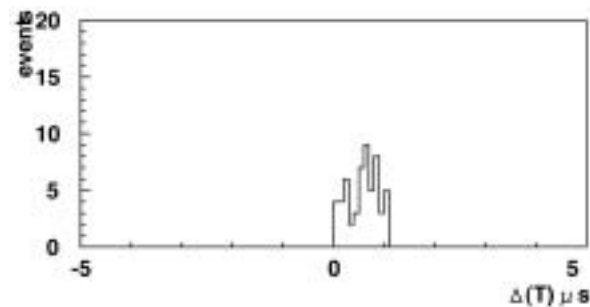


Fig. 16. The timing distribution of fully contained event observed at Super-Kamiokande with respect to the beam injection timing.

neutrino energy spectrum was obtained for the far detector. All the systematic errors due to detector bias or uncertainty of neutrino interactions were carefully taken into account. The neutrino beam was delivered about 6 months per year from 1999. We have accumulated 4.8×10^{19} protons from April 1999 to July 2001.

The synchronization of the timing between KEK 12 GeV Proton Synchrotron and Super-Kamiokande detector was performed using a GPS system. Figure 16 shows the timing distribution of the fully contained events observed at Super-Kamiokande with respect to the proton beam injection timing. The time of flight of neutrinos from KEK to Super-Kamiokande ($\sim 830 \mu\text{sec}$) is corrected in the figure.

Neutrino events were clearly observed near $\Delta T = 0$ and the spread in the timing was consistent with the duration of beam injection at KEK 12 GeV PS. In total, 56 events were identified as K2K beam induced events at Super-Kamiokande. Using the large number of observed neutrino events at front detectors, expected number of neutrino events at Super-Kamiokande was calculated to be $80.1^{+6.2}_{-5.4}$ assuming no-oscillation.

29 μ -like single ring events were observed and the neutrino energy spectrum obtained from the energy and scattering angle of the observed muons is shown in Fig. 17. From the deficit

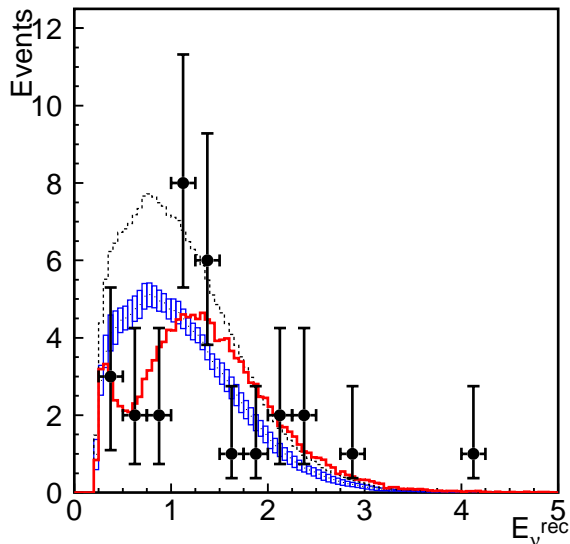


Fig. 17. The reconstructed E_ν distribution from single ring fully contained events at SK. Points with error bars are data. Box histogram is expected spectrum without oscillations, where the height of the box is the systematic error. The solid line is the best fit spectrum. These histograms are normalized by the number of events observed. In addition, the dashed line shows the expectation with no oscillations normalized to the expected number of events.

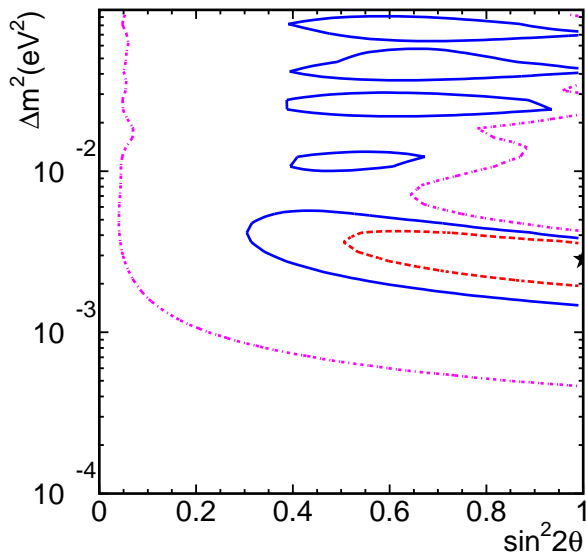


Fig. 18. Allowed regions of oscillation parameters. Dashed, solid and dot-dashed lines are 68.4%, 90% and 99% C.L. contours, respectively. The best fit point is indicated by the star.

of observed number of events together with the shape distortion of neutrino energy spectrum, we have concluded that probability of null oscillation is less than 1%. The allowed region of Δm^2 and $\sin^2 2\theta$ is shown in Fig. 18. The obtained result for neutrino oscillation parameters are consistent with that from atmospheric neutrino oscillations.

K2K is expected to continue accumulating data through early 2005. By that time, the number of neutrinos observed in Super-Kamiokande should be twice larger than at present, and statistically significant, detailed analysis of the neutrino

oscillations will be possible.

List of Publications

- [1] Ahn, S. H. et al. 2001, Detection of accelerator produced neutrinos at a distance of 250 km. *Phys. Lett. B*, 511, 178–184.
The number of citations: 87
- [2] Ahn, M. H. et al. 2002, Indication of neutrino oscillation in a 250 km long baseline experiment. *to be published in Phys. Rev. Lett.*

Collaboration

Institute	Country	(*)
ICRR, Univ. of Tokyo	Japan	23
KEK, High Energy Accelerator Research Organization	Japan	12
Kobe University	Japan	6
Kyoto University	Japan	8
Niigata University	Japan	2
Okayama University	Japan	3
Tokyo University of Science	Japan	1
Tohoku University	Japan	1
Chonnam University	Korea	5
Dongshin University	Korea	1
Korea University	Korea	1
Seoul National University	Korea	6
Boston University	USA	4
University of California at Irvine	USA	5
University of Hawaii at Manoa	USA	3
Massachusetts Institute of Technology	USA	1
State University of New York at Stony Brook	USA	6
University of Washington at Seattle	USA	3
University of Warsaw	Poland	2

(*) Number of participants.

μ - ν (Gravitational Wave)

Overview

• Gravitational wave experiment

Gravitational waves are physical entities in spacetime predicted by Einstein's theory of general relativity. Their existence was indirectly proven by the observation of PSR1913+16 by Taylor and Hulse¹ who won the Nobel prize in 1993. However, nobody has succeeded in directly detecting gravitational waves.

Theory of gravitation is tested by the detection of gravitational waves. A gravitational wave detector is the last eye of mankind to inspect the universe.

In order to directly observe gravitational waves, we have been developing a large scale interferometric gravitational wave detector. We succeeded in operating TAMA for more than 1000 hours with a sensitivity which would make observation of the coalescence of double neutron stars occurring within a range of 30 kpc with a signal to noise ratio of 10. After this long term observation, we installed a power recycling mirror to improve its sensitivity towards its final goal.

However, it is difficult to observe such gravitational wave events because statistical studies show that the birth rate of the coalescence of double neutron stars is 10^{-6} a year in a galaxy as big as our Galaxy.² This means that we need to wait for long time to detect the gravitational wave from the coalescence of binary neutron stars by the present detector. This is the reason why we have to construct LCGT (Large-scale Cryogenic Gravitational wave Telescope).³

There are many other possible gravitational wave sources in the universe other than the coalescence of binary neutron stars. However, the coalescence of binary neutron stars differs completely from other sources in the sense that its wave form is precisely determined and its existence is certainly confirmed.

LCGT adopts cryogenic mirrors with a 3 km baseline and will be mounted in tunnels in the Kamioka mine. We are conducting R&Ds for cryogenic mirrors and planing to build a 100 m cryogenic laser interferometer (CLIO) at the Kamioka site, which is promised to be financed for 2002–2006.

TAMA project

[Spokesperson : Kazuaki Kuroda]

μ - ν Div., ICRR, Univ. of Tokyo, Kashiwa, Chiba 277-8582

- ¹ J.H. Taylor and J.M. Weisberg, Further experimental tests of relativistic gravity using the binary pulsar PSR 1913+16, *Astrophysical J.*, **345** (1989) 434.
- ² E.S. Phinney, The rate of neutron star binary merges in the universe: minimal predictions for gravity wave detectors, *Astrophysical J.* **380** (1991) L17.
- ³ K. Kuroda, *et al.*, Large-scale cryogenic gravitational wave telescope, *Int. J. Mod. Phys.* **D8** (1999) 557.

Table 1. TAMA data taking runs.

Run	Term	Year	Length (Hour)
DT1	6-Aug → 7-Aug	1999	7
DT2	17-Sept → 20-Sept	1999	31
DT3	20-Apr → 23-Apr	2000	13
DT4	21-Aug → 4-Sept	2000	161
DT5	2-Mar → 8-Mar	2001	111
DT6	15-Aug → 20-Sept	2001	1038

In collaboration with members of :

TAMA collaboration (NAOJ, Tokyo; KEK, Tsukuba; UEC, Tokyo; Osaka City Univ., Osaka; Kyoto Univ., Kyoto; Osaka Univ., Osaka; Niigata Univ., Niigata)

TAMA is a gravitational wave project to construct a 300 m baseline laser interferometer at the Mitaka campus of the National Astronomical Observatory of Japan (NAOJ) and to conduct observations. TAMA is a five year project started in April, 1995 and is organized by researchers belonging to universities and national laboratories. We regard the TAMA interferometer as a step towards the final scale interferometer in the sense of technology and the construction budget. We have achieved so far six data taking runs that spans from two to four weeks (Table 1). In the former half runs, its sensitivity improvement was the first priority. Nonetheless, both stability and reliability needed to be improved to check the sensitivity itself. In the latter half runs, the operation became easier by the installation of an automatic control system.

During the course of this project, we have established techniques necessary for constructing large-scale and highly sensitive interferometers. We are confident that the TAMA project is successful and that the several techniques developed so far will be useful for LCGT in the future.

The data taken at DT6 is under study. No traces of gravitational waves have been detected. Previous result was published and its stable operation was reported.⁴ The sensitivity of each run is shown in Fig. 1 (the dates do not exactly correspond to those of data taking runs). The sensitivity has been steadily improved and is close to the goal of the first phase (the first phase means the interferometer optical system without a recycling mirror).

At the time of DT6, we analyzed several noise sources that governed the sensitivity curve and almost all sources

- ⁴ H. Tagoshi, *et al.*, First search for gravitational waves from inspiraling compact binaries using TAMA300 data, *Phys. Rev.* **D63** (2001) 062001-1; M. Ando, *et al.*, Stable operation of a 300-m Laser Interferometer with Sufficient Sensitivity to Detect Gravitational-Wave Events within Our Galaxy, *Phys. Rev. Lett.* **86** (2001) 3950.

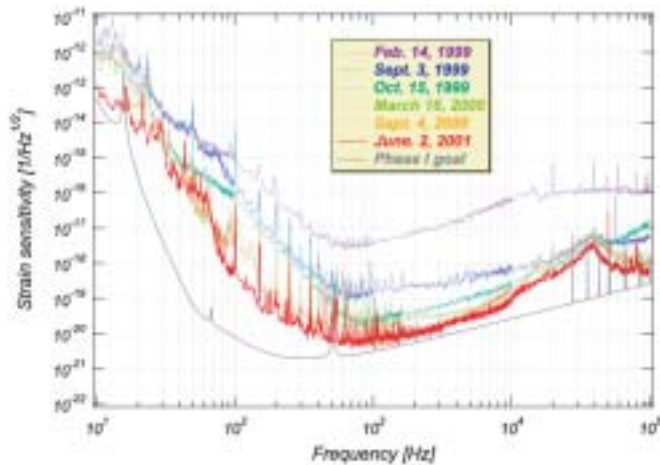


Fig. 1. TAMA sensitivity is steadily improved. It is close to the goal sensitivity of the first phase.

were identified except the noise that limits the sensitivity around at 600 Hz.

After DT6, TAMA entered a Phase II stage, where a power recycling mirror was installed to reduce the shot noise. The recycling mirror was installed between the beam splitter and the mode cleaner (in Fig. 2). At this stage, the power recycling gain was set three, that will be finally set 10. The sensitivity was not recovered to the level of DT6 in this financial year, mainly due to a total rearrangement of optical pieces.

We could observe the coalescence of neutron star binaries occurring within 30 kpc with a signal to noise ratio of 10 at the time of DT6. The range depends on the mass of the target as shown in Fig. 3. As far as the coalescence of the binary neutron stars with the nominal mass of $1.4 M_{\odot}$ is concerned, the distance range does not become larger by improving the sensitivity at lower frequency such as 100 Hz. Low frequency improvement is effective for the detection of coalescences involving heavier compact star like black holes. Roughly speaking, the final goal would be attained by raising the sensitivity by ten. This can be performed by increasing internal light power by applying the power recycling.

R&D for LCGT

[Spokesperson : Kazuaki Kuroda]

μ - ν Div., ICRR, Univ. of Tokyo, Kashiwa, Chiba 277-8582

In collaboration with members of :

LCGT collaboration (NAOJ, Tokyo; KEK, Tsukuba; UEC, Tokyo; Osaka City Univ., Osaka; Kyoto Univ., Kyoto; Osaka Univ., Osaka; Niigata Univ., Niigata)

The target sensitivity of LCGT is to observe binary neutron star coalescence events occurring at 200 Mpc with $S/N=10$. This is ten times more sensitive than that of the first LIGO and two orders more than that of TAMA at their most sensitive frequencies. This will

be attained by using a three-kilometer baseline located underground, cooling mirrors at cryogenic temperature, and high-power laser source employing a 100 W output with higher recycling gain. The optical configuration succeeds that of TAMA, which is a Fabry-Perot-Michelson interferometer with techniques of the frontal modulation, wave-front sensing, and power recycling.

The Table 2 lists the important parameters of LCGT. The ultimate sensitivity of a laser interferometer is determined by seismic noise at low frequency (10–30 Hz) (which is reduced by improving the vibrational isolation system), and it is limited by photon shot noise at high frequency (more than 300 Hz), which can be improved only by increasing the light power in the main cavities. The sensitivity of middle frequencies (30–300 Hz) is limited by thermal noise and this is reduced both by decreasing the temperature and by decreasing the internal mechanical loss (*i.e.*, increasing the mechanical Q of vibrational modes). The source of thermal noise comes from both mirror internal vibration and swing noise of the pendulum supporting the mirror. Reduction of thermal noise is attained by cooling down the temperature of both the mirror itself and the suspension system that suspends the mirror.

The main effort on the research and development for LCGT has been placed on cryogenic mirrors for the past years. The implementation of cryogenic mirrors is one of the most straight forward solutions for the improvement of sensitivity.

A conceptual design of the cryogenic mirror system is shown in Fig. 4, where only part of the end-mirror chamber is focused. The mirror is suspended by one or two loops of sapphire fibers connected to an alignment control platform that has a heat link to the heat anchor (4 K) inside the vacuum located just above the platform. This platform is suspended with a G-10 (thermal insulator) rod connected through the center holes of the radiation shields to an isolation table suspended by a low frequency vibration isolator, which is at room temperature. All of these cryogenic system and the vibration isolator are put inside the common high vacuum. The support of the vibration isolator needs to be fixed on the ground independently of the chamber supports (Figure 4 differently shows).

To realize this concept, the following research subjects were considered:

1. removal of the heat produced by high power laser illumination
2. maintenance of the high Qs of mirror internal modes and suspension pendulum
3. prevention of contamination of mirror surfaces
4. estimation of heat production by optical loss in the mirror
5. control of the alignment of mirrors in cryogenic environment

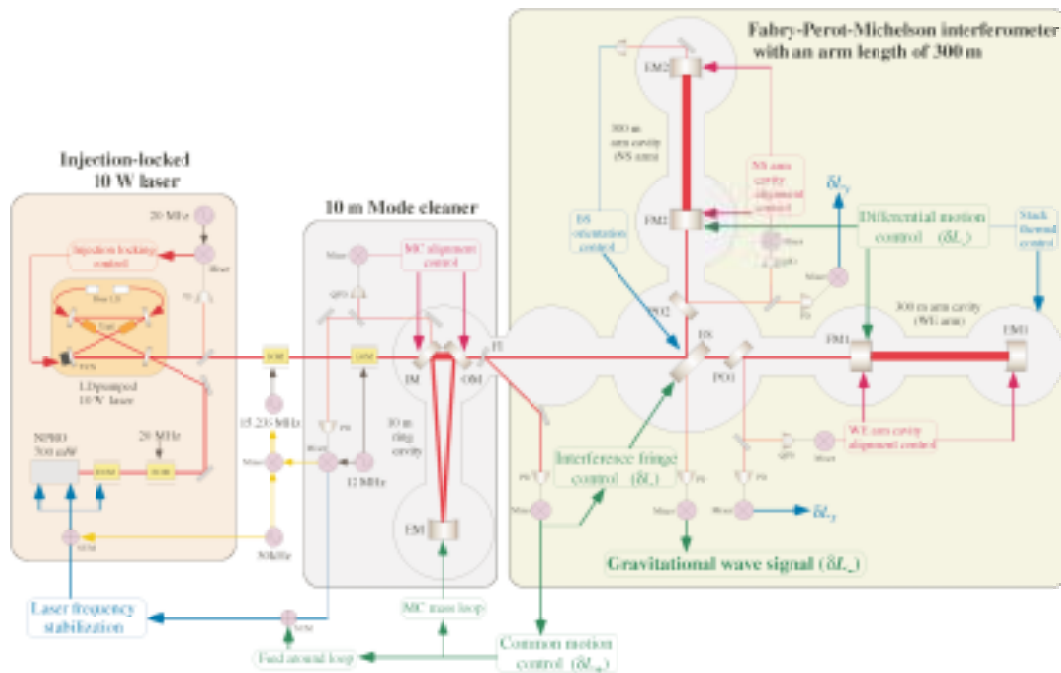


Fig. 2. Optical configuration of TAMA300 at the time of DT6. After DT6 the recycling mirror was installed between the beam splitter and the mode cleaner.

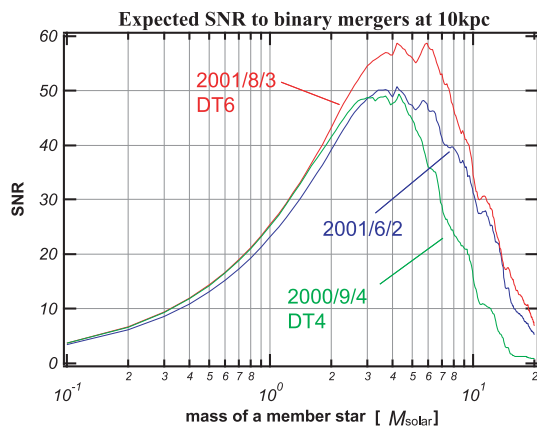


Fig. 3. Expected signal to noise (SN) ratio for each mass of detectable binary system at 10 kpc. The sensitivity at 100 Hz was better at the time of DT6 than in June, 2001. This improved SN ratio for heavier mass of the member star of binaries. The improvement at the mass of the neutron star binary ($1.4 M_{\odot}$) was relatively small.

Table 2. LCGT design parameters

Item	Parameter
Baseline Length	3 km
Laser Power	100 W
Input power at BS	1 kW
Finesse of main cavity	1250
Beam radius at End	3 cm
Main Mirror	Sapphire 51 kg, 30 K
Mechanical Q	10^8
Suspension pendulum	1 Hz, $Q=2 \times 10^8$, 10 K
Anti-vibration	10^{-3} at 1 Hz

We had already finished the first two subjects and had reported in the previous annual report (1997–1998).⁵

In regard to the third and fourth items, the results were reported in the last annual report (2000–2001) and published in papers.⁶

⁵ T. Uchiyama, *et al.*, Cryogenic cooling of a sapphire mirror-suspension for interferometric gravitational wave detectors, *Phys. Lett.* **A242** (1998) 211; T. Uchiyama, *et al.*, Mechanical quality factor of a cryogenic sapphire test mass for gravitational wave detectors, *Phys. Lett.* **A261** (1999) 5; T. Uchiyama, *et al.*, Mechanical quality factor of a sapphire fiber at cryogenic temperatures, *Phys. Lett.* **A273** (2000) 310.

⁶ S. Miyoki, *et al.*, Cryogenic contamination of an ultra-low loss

As for the last item, we confirmed that a superconducting film can be used for the receptor of magnetic force in place of permanent bar magnets that are normally used in the existing detectors. The film can be easily sputtered on the mirror surface without harmfully degrading the mechanical Q of the mirror.

All the above R&Ds confirmed the feasibility of the reduction of thermal noise of the interferometer. We evaluated that these researches underline the basis of LCGT. However, a practical cryogenic detector need many prac-

mirror for cryogenic laser interferometric gravitational wave detector, *Cryogenics* **40** (2000) 61; S. Miyoki, *et al.*, Cryogenic contamination speed for cryogenic laser interferometric gravitational wave detector, *Cryogenics* **41** (2001) 415; T. Tomaru, *et al.*, Cryogenic measurement of the optical absorption coefficient in sapphire crystals at $1.064 \mu\text{m}$ for the large-scale cryogenic gravitational wave telescope, *Phys. Lett.* **A283** (2001) 80.

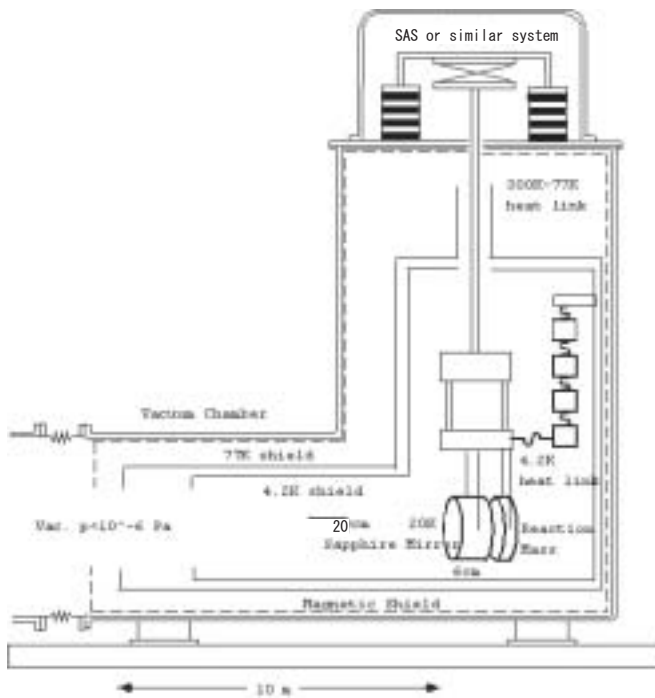


Fig. 4. Overview of the cryogenic suspension system. The mirror is suspended by sapphire fibers connected to a platform that has a heat link to a 4 K heat anchor inside the vacuum. The platform is suspended with a G-10 rod connected through the center holes of radiation shields to an isolation table suspended by low frequency anti-vibration system at room temperature in the common high vacuum.

tical R&Ds for the installation of cryogenic mirrors. Therefore, we started to do researches for this application. The next section describes one of such R&Ds.

A dependence of thermal conductivity on thickness of fiber

The mirror is cooled by sapphire crystalline fibers. The conductivity test had been done using 250 μm diameter sapphire fibers. The diameter of the fiber was chosen by the consideration of the bending curvature that could tightly wrap the cylindrical surface of the mirror, 10 cm in diameter. Since the mirror size is increased up to 20–30 cm for LCGT, we can adopt thicker fibers. Although the suspension thermal noise limits the thickness of the fiber at room temperature, the sapphire suspension becomes free from this limit at cryogenic temperature mainly due to a decreasing thermal expansion rate towards lower temperatures. Therefore, thicker fiber can be used to satisfy the sole requirement of heat flow from the mirror to the heat anchor point. If the diameter of the fibers are increased, thermal conductivity at cryogenic temperature supposedly increase more rapidly than the square of the diameter because of the ease of phonon scattering at the inner surface of the fiber so long as the diameter is shorter than the mean free path of phonons at the temperature.

Experiment to check this point was done by measuring conductivities of three kinds of diameter and the depen-

Fig. 5. Thermal conductivity of sapphire fiber was found to be proportional to its cubic of the diameter for thin fibers.

dence was found to be proportional to the cubic of the diameter (Fig. 5). This result reduces the load of sapphire fibers in consideration of the heat flow.

In regard to the last question of the actuation at cryogenic temperature, we are developing an actuation method that utilizes Meissner effect in a thin superconducting film on the surface of the mirror. This magnetic actuator has wider dynamic range compared with electrostatic actuation method. A practical design must be pursued for LCGT.

R&D research in Kashiwa

To show the feasibility of cryogenic mirrors for more sensitive detectors, a cryogenic interferometer needs to be established. For this purpose we are developing a one-arm cryogenic interferometer. A vacuum cryostat system with a beam duct was made and set in Kashiwa campus. It has two identical vacuum cryostats and a 6 m long vacuum tube with radiation shield (40 K) inside. In this cryostat, the cylindrical axis of radiation shields and also that of the vacuum chamber are placed horizontally. We can access the experimental inner space by horizontally opening the vacuum lids. Cryogenic temperatures are maintained by a Gifford-McMahon refrigerator with thermal conductor from the head of the refrigerator to the inner radiation shield. Since the refrigerator is a vibration noise source, it is designed to be mounted far from the cryostat itself.

Cooling speed and mechanical vibration were measured and compared with their design values as reported in the previous annual report. For the cooling speed, since the design was done for steady state in cryogenic temperature, the low thermal conductivity of the thermal conductor in higher temperature caused a fairly long cooling time, roughly one week. However, this long cooling time is compensated by ease of use of the cryostat system. Because this system does not need liquid nitro-

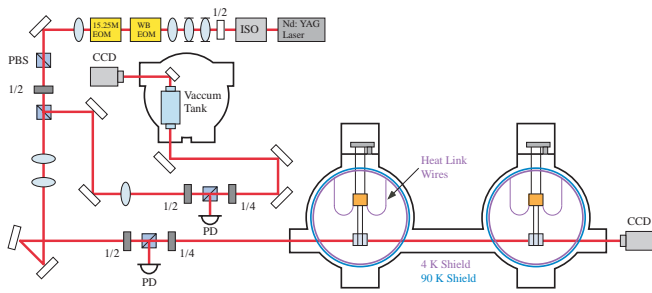


Fig. 6. Experiment for Cryogenic mirror suspension system in Kashiwa campus. One arm Fabry-Perot cavity consists of two cryogenic mirrors housed in cryostats connecting 6 m long vacuum tube with inner radiation shield. Optical system needs to be put inside the vacuum to reduce sound noise.



Fig. 8. 20 m interferometer in Kamioka Mine

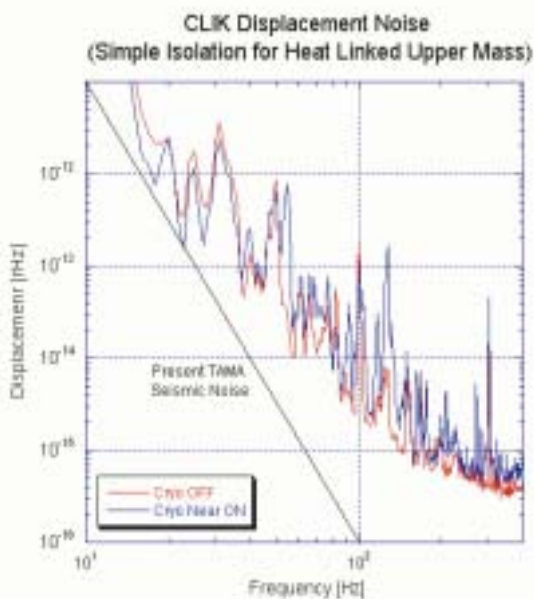


Fig. 7. Disturbance of the refrigerator vibration at the suspended mirrors of the cryogenic Fabry-Perot interferometer.

gen nor liquid helium.

An optical layout of the experiment is shown in Fig. 6. The effect of the vibration of the refrigerators was low enough to be isolated by conventional anti-vibration technique as designed. The measured displacement noise is shown in Fig. 7. The excitation around 50 Hz in this figure was thought to be produced by the mechanical resonances of the radiation shield plates, which can be reduced by appropriate support stems inside the cryostat chamber in the next experiment.

In conclusion, we have succeeded to present the feasibility of using cryogenic mirrors for LCGT by the above basic experiments in the past years. The next step in R&D for cryogenic mirrors is to show the reduction of noise amplitude itself, which needs more realistic interferometer other than the prototype with a shorter base-

line.

Kamioka 20 m prototype detector for possible coalescence of binary MACHO

[Spokesperson : Masatake Ohashi]

μ - ν Div., ICRR, Univ. of Tokyo, Kashiwa, Chiba 277-8582

In collaboration with members of :
NAOJ, Tokyo; NIAIST, Tsukuba

The prototype 20 m interferometer (LISM) was operated underground of the Kamioka Mine. The site near the Super-Kamiokande detector is a planned site of LCGT. The LISM has shown a long term stability of the interferometer and produced a high-quality data by taking advantage of both the low seismic noise and the high temperature stability in the Kamioka underground space.

We developed the 20 m prototype interferometer at NAOJ since 1991. When the final experiment for R&D of TAMA project (a high-gain recycling⁷) was finished, we decided to move the 20 m interferometer from TAMA site into the Kamioka Mine to catch possible GW events from the coalescence of binary MACHO-BHs in our Galaxy⁸.

LISM interferometer consists of three parts; a light source with a mode cleaner, a primary cavity as a frequency reference and a secondary cavity to sense GW. A laser is a commercial NPRO with wavelength of 1064 nm and output power of 700 mW. Two cavity are formed by a pair of high quality mirrors with a finesse of about 25000 and length of 20 m. The optical layout is called as Locked Fabry-Perot configuration (shown in Fig. 9). The main part of LISM is housed in vacuum chambers and the pressure is kept at 10^{-6} torr by two ion pumps. Data acquisition system has eight channels with 20 kHz sampling and another eight channels with slow sampling for monitoring the interferometer and environment. Time information is obtained from GPS signals. We started

⁷ S. Sato, *et al.*, Applied Optics, **39** (2000) 4616–4620.

⁸ T. Nakamura, *et al.*, ApJ **487** (1997), L139.

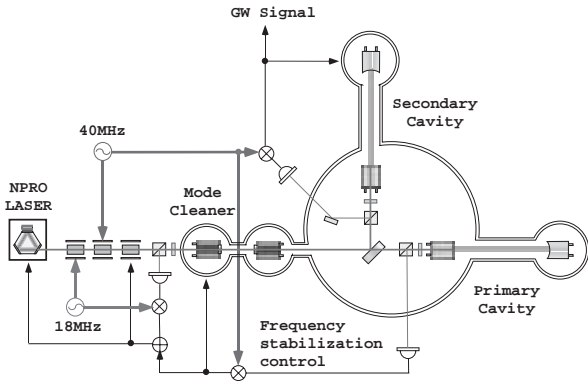


Fig. 9. Optical layout of LISM interferometer

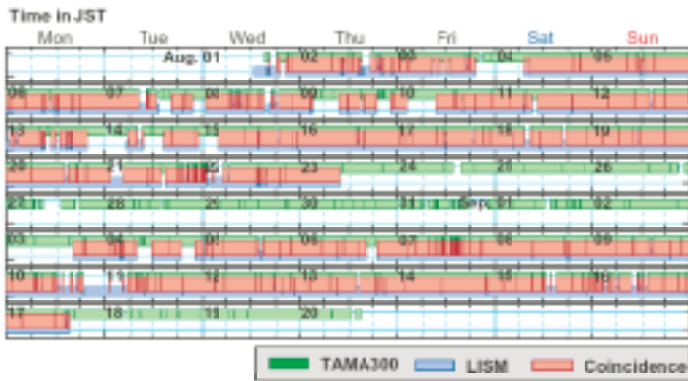


Fig. 10. Lock Status Summary of TAMA300 and LISM

observations early in 2000. The operation of LISM is very stable owing to the advantage of quiet underground site.

After several improvements, mainly frequency stabilization of the laser, the strain sensitivity of LISM reached $h_{\text{rms}} = 6.0 \times 10^{-20}$ around 800 Hz. This sensitivity makes it possible to catch the event of binary neutron star inspirals up to 1kpc with SN=10. A coincidence run with TAMA300 is highly important. We synchronized LISM observation with DT6 of TAMA300 (Fig. 10). Over 700 hours data were recorded and the analysis is now underway. This is a first coincidence analysis of actual two interferometers in the world.

SDSS

SLOAN DIGITAL SKY SURVEY

The Sloan Digital Sky Survey (SDSS) achieved the *Photometric First Light* in May 1998. It began to take commissioning data from the fall of the same year. During the time the construction of the two double spectrographs was completed and the first observation was made in May 1999. Since then both hardware and software have been tuned and the quality of the data have been brought into nearly the survey grade. While we are still in the beginning of the survey and we still need to understand some systematics, as well as to improve the calibration, the data we obtained by now greatly surpass the standard of currently available wide field surveys in both quality and quantity, but also in the photometric precision. As for the quantity, it would be enough to mention that imaging over 150 square degrees is carried out with five colours in one night, which is compared to a typical ‘wide field survey’ that comprises a few square degrees with one, or at most, two colours. Photometric surveys which are comparable to SDSS in the sky coverage all use photographic plates. A typical example is Anglo-Australian project 2dF, whose photometric accuracy is no better than 30%, which is compared to 2–3% accuracy of the SDSS. This achievement is clearly by virtue of the huge CCD camera we have built. We select target objects for spectroscopy based on the photometric survey, so that the photometric accuracy limits the fundamental accuracy of all follow-up observations and analyses. The SDSS also enjoys an enormous spectroscopic capability. We are able to obtain over 6000 spectra per night if we spend a full night for spectroscopy. Our operations are not yet at the full scale, since we still need many verifications. By the spring of 2001, however, 6% of the sky (2,400 square degrees) have been imaged and 3% of the sky (150,000 spectra) are spectroscopically studied. (Our goal is to survey over 1/4 the entire sky).

These data have been used to produce early science results. By the time of the end of FY2000, 25 papers have been written for research journals and 14 have already been published; these numbers are rapidly growing at the time of writing this report. The topics cover wide subjects of astronomy, stellar science, galaxy science, active galactic nuclei, and cosmology. Specifically, enormous multi-colour imaging capability has greatly pushed forward high redshift quasar studies. This is demonstrated by the number of high redshift quasars we have found: 40 years of quasar searches have given 105 quasars with redshifts (z) higher than 4; From 10 nights of imaging SDSS found 132 quasars with $z > 4$. For $z > 5$ 10 out of 11 are SDSS quasars. The highest redshift record was renewed 4 times, and now it is $z = 6.3$. It is interesting that these quasars show normal spectra, indicating the presence of the normal heavy element abundance. Our study has enabled to delineate the evolution of quasars

when galaxies were forming. We have also discovered a strange ‘quasar’ which does not show any emission lines.

We have found a number of low temperature stars, which are beyond M type and classified as L and T types. T stars are dominated by methane absorption bands, quite similar to the Jupiter spectrum. It was shown that L and T stars form a continuous class in spite of an apparent discontinuity observed in the optical colour bands. These observations have already promoted studies of the atmosphere of low temperature stars where the dust forms. From the observed number density of these low temperature stars we can conclude that low mass stars do not dominate the stellar mass of galaxies, as was once conjectured to solve the dark matter problem. Studies of stars are interesting not only from their own right, but also in that they would shed light on the structure of Milky Way. An analysis of the colour-magnitude diagram for millions of stars we imaged has revealed that the thin Galactic disc (to which the sun belongs to) is surrounded by a thick disc of the scale height twice the thin disc. These thick disc stars are clearly distinguished from halo stars. The presence of the thick disc has been suggested for a decade but it has been a matter of debate: the SDSS established its presence unambiguously. We have also assembled a large number of RR Lyrae, from which we could show that halo stars are distributed as $r^{-2.7}$ out to 60 kpc from the Galactic centre, but their distribution sharply declines beyond this distance: the Milky Way has a sharp edge. This study at the same time revealed a conspicuous clump of stars at 50 kpc from the Galactic centre. A further study of the spatial distribution of A stars showed that this clump is interpreted as debris from the collision of the Sagittarius dwarf galaxy with the Milky Way. These are all important aspects to understand how galaxies formed and evolved.

Galaxy science needed more time to produce results, as we had to first verify the quality of catalogues. For this purpose we have inspected more than 100,000 objects by eyes and checked against catalogues produced by the photometric pipeline. This effort has clarified the statistical accuracy of the galaxy catalogue, but also it has been used to tune the software. One of the most elementary analyses for galaxy science is galaxy counts as a function of magnitude. We have derived the counts from one million galaxies for a range over 10 magnitudes, from 12 to 22 mag, much wider in the dynamic range than any other single surveys to date could explore. This study showed that the counts behave as expected in a homogeneous universe, excluding a few indications for the contrary made in the past. At the same time, however, we have detected a small variation of the galaxy distribution over a very large scale (which affects up to 150 Mpc). An accurate determination of the luminosity function of galaxies in five colour bands have also a great impact on

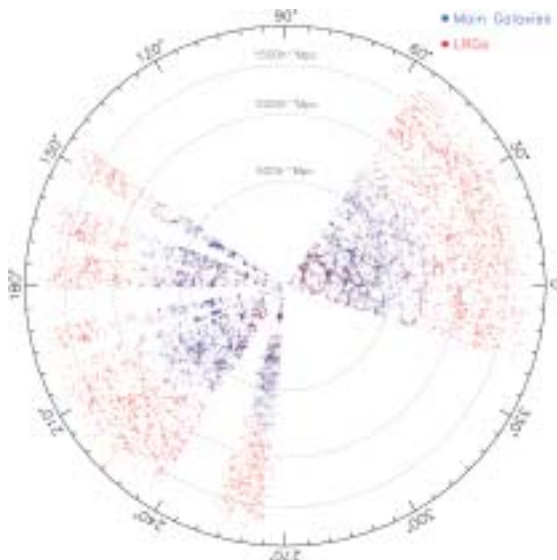


Fig. 1. 'Pie diagram': a section of the three dimensional distribution of galaxies in the (2.5 deg wide) equatorial strip. The data contains about 40,000 galaxies obtained in 4 nights of imaging and 10 nights of spectroscopic follow-up. The black points stand for normal galaxies to $r' = 17.8$ mag, and red points are luminous red galaxies to $r' = 18.8$ mag in order to sample a deeper sky. Note that the limit of the celebrated Harvard Center for Astrophysics survey is about 150 Mpc.

galaxy science, since it is the most fundamental statistic that is used for any statistical analyses of galaxies, yet has suffered from uncertainties by a factor of two in the normalisation. This uncertainty has hampered accurate understanding of evolution of galaxies.

SDSS is among a few groups which detected the gravitational lensing shear field caused by galaxies at the first time. The shear from individual galaxies is very small and this detection needed a large statistical sample. Taking the advantage that lensing galaxies of the SDSS sample are given redshift measurements we could determine the mass to light ratio of galaxies, which is about 150 in solar units out to a large radius ($\sim 260h^{-1}$ kpc).

The quantitative understanding of large-scale structure of the universe is one of the advertised goals of the SDSS project. We have just started studies for large-scale clustering of galaxies. Our current aim is to clarify systematic effects, to establish the robust strategy to derive the power spectrum of density perturbations, and to estimate the realistic error of the analysis. We have employed several independent methods to derive the power spectrum, and verified that all methods give a convergent answer where they ought to do if proper treatments are made for the data.

There are many more to write about science from SDSS, but we should quit here. Many objects found by SDSS have already been taken as excellent targets of observations for more detailed studies with the Subaru Telescope from its beginning phase. We finally advertise that our data taken at the equatorial strips (for both north and south, 2.5 deg wide) are already open to the public (from June 2000). The data are 5% of the goal, but many millions of objects are registered in the cata-

logue. We note, however, that the catalogue in the state of the art is not quite complete, and the users are advised to verify it appropriately before their use.

AIR SHOWER DIVISION

Overview

Two major research activities of the Air Shower division are the study of extremely high energy cosmic rays by the AGASA/TA group and very high energy gamma rays by the CANGAROO group.

At the Akeno observatory, a series of air shower arrays of increasing geometrical sizes have been constructed and operated to observe ultra high energy cosmic rays. The AGASA (Akeno Giant Air Shower Array) is the newest and the largest, which started the operation in 1991 and presently covers the ground area of 100 km² as the world largest air shower array. In 10 years of operation, AGASA observed a handful of cosmic rays exceeding the theoretical energy end point of the extra-galactic cosmic rays (GZK cutoff) at 10²⁰ eV. The Telescope Array (TA), an array of air fluorescence telescopes to be built in Utah, USA, is to succeed the AGASA with 30 times larger aperture and the particle identification capability. It intends to unveil the origin of super-GZK cosmic rays discovered by the AGASA.

The CANGAROO project (Collaboration of Australia and Nippon for a Gamma-Ray Observatory in the Outback) is a set of large imaging Cherenkov telescopes to make a precise observation of high-energy air showers originated by TeV gamma-rays. It started as a single telescope with a relatively small mirror (3.8 m in diameter) in 1992. In 1999 a new telescope with a 7-m reflector has been built, and now it has a 10-m reflector with a fine pixel camera. The main purpose of this project is to explore the violent, non-thermal universe and to reveal the origin of cosmic-rays. We have detected several gamma-ray sources in the southern sky and detailed study of these sources are now ongoing.

Study of the Most Energetic Cosmic Rays with AGASA — AGASA Collaboration

[Spokesperson : M. Teshima]

Air Shower Div. ICRR, Univ. of Tokyo, Kashiwa, Chiba 277-8582

In collaboration with the members of:

Hirosaki University, Hirosaki; Saitama University, Urawa; Tokyo Institute of Technology, Tokyo; Nishina Memorial Foundation, Tokyo; Yamanashi University, Kofu; Nagoya University, Nagoya; Ehime University, Matsuyama; Osaka City University, Osaka; Fukui University of Technology, Fukui; National Institute of Radiological Sciences, Chiba; RIKEN, Saitama.

1. Introduction

AGASA [1, 2] is the Akeno Giant Air Shower Array covering over 100 km² area in operation at Akeno village about 130 km west of Tokyo, in order to study extremely high energy cosmic rays (EHECR) above 10¹⁹ eV. In this energy region, distinctive features in the energy spectrum and arrival direction distribution are expected.

If the cosmic rays are of extragalactic origin, photopion production between cosmic rays and primordial microwave background photons becomes important at energies above 6×10^{19} eV with a mean free path of about 6 Mpc. Therefore a cutoff in the spectrum are expected around several times 10¹⁹ eV. This is called as the Greisen-Zatsepin-Kuzmin (GZK) cutoff [3]. Since the cosmic rays exceeding this cutoff energy must be originated at nearby sources within 50 Mpc. In this scenario, the expected arrival direction distribution of EHECR is relatively isotropic and should have some correlation with the material distribution around our galaxy; super galactic plane or clusters of galaxies.

On the other hand, if they are galactic origin, their arrival direction distribution should have strong correlation with the galactic structure, since the gyroradius of protons of energy above 10¹⁹ eV are comparable with the galactic scale. Therefore a study of correlations of EHECR with the galactic structure and/or with the large scale structure of galaxies is important.

As acceleration mechanism of these EHECR, the diffusive shock acceleration is most widely accepted and shocks at radio lobes of relativistic jets from Active Galactic Nuclei, termination shocks in local group of galaxies, etc. are discussed to be possible sites [4]. The acceleration above 10²⁰ eV in dissipative wind models of cosmological gamma-ray burst is also proposed [5]. Since various difficulties are still anticipated in accelerating cosmic rays up to the highest observed energies, it is also discussed that these cosmic rays are possibly the decay products of some massive particles produced at the collapse and/or annihilation of cosmic topological defects which could have been formed in a symmetry-breaking phase transition in the early universe [6].

The details of the AGASA are described in Chiba et al. [1] and Ohoka et al. [2]. The array is operational since 1991 and the exposure is about 1500 km² sr year till the end of 2000. Extensive air showers, observed till July 2001, with zenith angles smaller than 45° and with core locations inside the array area were used. In the energy range above 10¹⁹ eV, we only used such events that passed through an eye scan to confirm their core positions and energies.

2. Energy Spectrum

In order to estimate the primary energy of giant air showers observed by the AGASA, the particle density at a distance of 600 m from the shower axis ($S(600)$) is used as an energy estimator, which is known to be a good parameter [7]. The conversion factor from $S(600)$ [per m^2] to primary energy E_0 [eV] is derived by simulation [8] as

$$E_0 = 2.0 \times 10^{17} \times S(600)^{1.0}. \quad (1)$$

The details of determination of arrival directions and $S(600)$ are described in Takeda et al. [10].

The differential primary energy spectra above $10^{18.5}$ eV are shown in Fig. 1 [10]. The bars represent statistical errors only and the error in the energy determination is about 30% above 10^{19} eV, which is estimated from analyzing the artificial showers simulated considering shower development fluctuation and experimental errors in each detector [10].

The energy spectrum extends beyond 10^{20} eV and we observed 8 events above GZK cutoff energy. If the real energy spectrum is that shown in Fig. 1 as the dashed curve, the expected number of events above 10^{20} eV is less than one, taking account of the energy resolution. The energy spectrum is therefore more likely to extend beyond 10^{20} eV without the GZK cutoff.

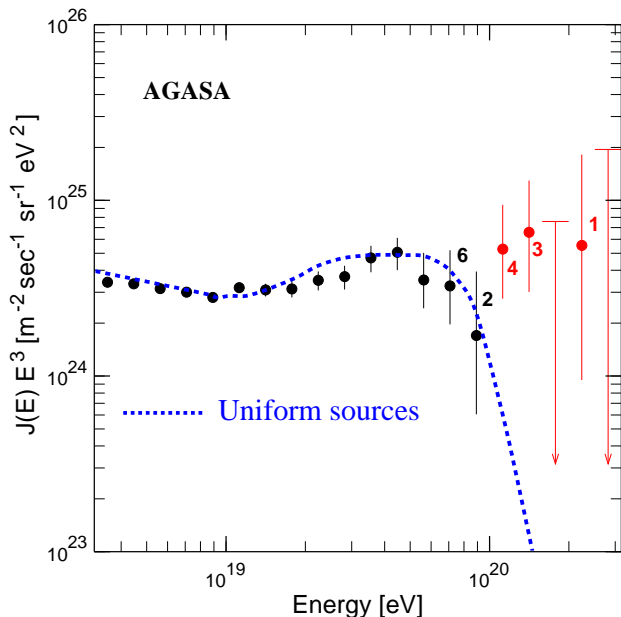


Fig. 1. The energy spectrum observed with AGASA. The vertical axis is multiplied by E^3 . Error bars represent the Poisson upper and lower limits at 68% and arrows are 90% C.L. upper limits. Numbers attached to points show the number of events in each energy bin. The dashed curve represents the spectrum expected for extragalactic sources distributed uniformly in the Universe, taking account of the energy determination error.

3. Arrival Direction

3.1 Above GZK energy

The arrival direction of the highest energy cosmic rays above 4×10^{19} eV is shown in Fig. 2 in the equatorial

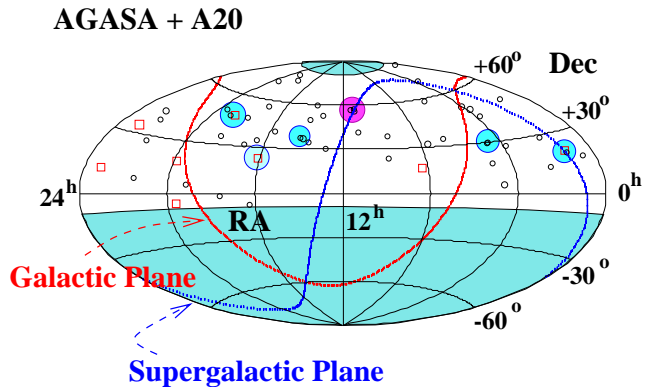


Fig. 2. The arrival direction of the highest energy cosmic rays above 10^{20} eV on the galactic coordinate.

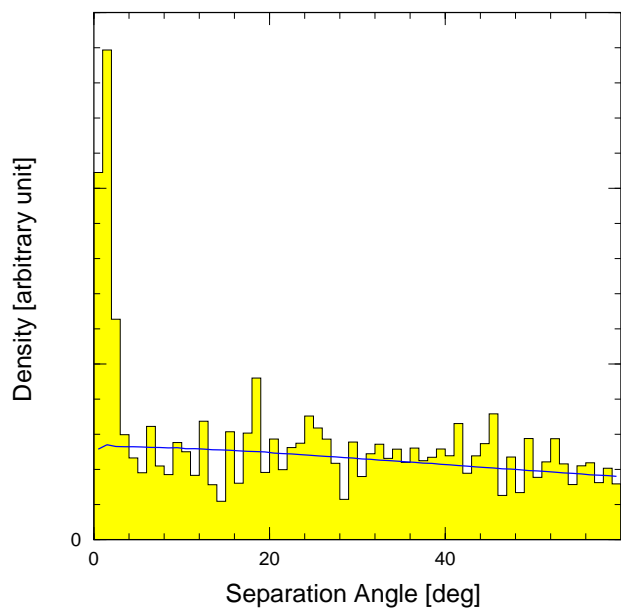


Fig. 3. The space angle distribution between two events above 4×10^{19} eV. We can see a clear peak below three degrees.

coordinate. Small dots and squares show events between 4×10^{19} eV and 10^{20} eV, respectively. They appear to be distributed uniformly over the observable sky. We have carried out several tests for global anisotropy but could not find any large scale structures in this distribution. However, we found one triplet and five doublets of events clustering within an angular resolution (2.5°) as indicated by shadowed circles. The chance probability for this clustering effect was evaluated as low as $P_{ch} \sim 10^{-3}$. No outstanding astronomical objects have been found in the directions of these clusters within 50 Mpc.

In Fig. 3, we have shown the space angle distribution between events (some kind of auto-correlation). We can see clear peak at small angles (≤ 3 degrees). This peak distribution could be explained by the angular resolution of AGASA. This result strongly suggests the existence of point like sources (compact sources) and weak magnetic

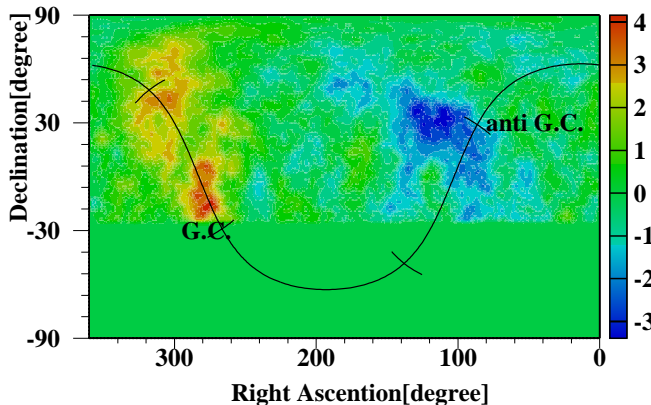


Fig. 4. The statistical significance of the deviations of the arrival direction distribution of the cosmic rays above 10^{18} eV on the equatorial coordinate.

field in the intergalactic spaces of $\leq nG$ order, if they are charged particles.

3.2 Anisotropy around 10^{18} eV

The harmonic analysis in the right ascension was carried out using the cosmic rays about 216,000 events observed by AGASA [11]. $k \sim 14$ at 10^{18} eV can be seen in the first harmonic. The phase of maximum amplitude corresponds to 15 hr in right ascension. The statistical significance is high, corresponding to a chance probability of 10^{-6} .

In Fig. 4 the arrival direction distributions in equatorial coordinates are shown. They show the statistical significance of the deviations from the expectation. Here, the energy region of 10^{18} eV $\sim 10^{18.4}$ eV is selected which maximize the harmonic analysis k -value. We can not observe events with declination less than -25° , as long as we use showers with zenith angles less than 60° . In this figure, we have chosen a circle of 20° radius to evaluate the excess. In the significance map, a 4.5σ excess (obs./exp. = 506/413.6) near the Galactic center region can be seen. In contrast, near the direction of anti-Galactic Center we can see a deficit in the cosmic ray intensity (-4.0σ). An event excess from the direction of the Cygnus region is also seen with 3.9σ (obs./exp. = 3401/3148).

4. The highest energy events

There are eight events whose energies exceed considerably the GZK cut-off energy. Their sources can't be very far and must be within a few tens of Mpc. However, there are no candidate astronomical objects within a few tens of Mpc in the direction of the highest energy events which may be able to accelerate particles to more than 10^{20} eV.

These observations have led to suggestions that particles may be directly produced by decay from objects produced in phenomenon occurring on a higher energy scale [6, 12]. For example, topological defects (TD's) left over from the phase transitions in the early uni-

verse, caused by the spontaneous breaking of symmetries, have been proposed as a candidate for production of extremely high energy cosmic rays. Such TD's are magnetic monopoles, cosmic strings, domain walls, superconducting strings etc. The remarkable result from this scenario is that bulk of cosmic rays above 10^{20} eV may be gamma-rays rather than protons and the energy spectrum is expected to extend up to the GUT scale $\sim 10^{25}$ eV with a hard exponent such as 1.35 [12], which is based on the exponent of hadronization in QCD.

References

- [1] N. Chiba et al., *Nucl. Instrum. Methods A* **311**, 388 (1992).
- [2] H. Ohoka et al., *Nucl. Instrum. Methods A* **A372**, 527 (1997).
- [3] K. Greisen, *Phys. Rev. Lett.* **16**, 748 (1966); G.T. Zatsepin and V.A. Kuzmin, *Pisma Zh. Eksp. Teor. Fiz.* **4**, 144 (1966).
- [4] Various acceleration models are discussed in *Astrophysical Aspects of the Most Energetic Cosmic Rays*, ed. M. Nagano and F. Takahara (World Scientific, Singapore, 1990) pp. 252–334.
- [5] E. Waxman, *Phys. Rev. Lett.* **75**, 386 (1995); M. Vietri, *Ap. J.* **453**, 883 (1995); M. Milgrom and V. Usov, *Ap. J.* **449**, L37 (1995);
- [6] Recent summary and references are described in P. Bhattacharjee, *Proc. of ICRR Symp. on Extremely High Energy Cosmic Rays : Astrophysics and Future Observatories* ed. M. Nagano, (Inst. of Cosmic Ray Research, University of Tokyo., 1997) p. 125.
- [7] A.M. Hillas et al, *Proc. 12th ICRC, Hobart* **3**, 1001 (1971).
- [8] H.Y. Dai et al., *J. Phys. G: Nucl. Part. Phys.* **14**, 793 (1988).
- [9] S. Yoshida et al., *J. Phys. G: Nucl. Part. Phys.* **20**, 651 (1994).
- [10] M. Takeda et al., *Phys. Rev. Lett.* **81**, 1163 (1998).
- [11] N. Hayashida et al., *Astroparticle Phys.* **10**, 303 (1999).
- [12] P. Bhattacharjee, C.T. Hill and D.N. Schramm, *Phys. Rev. Lett.* **69**, 567 (1992).

Telescope Array Project

[Spokesperson: M. Fukushima]

Air Shower Div. ICRR, Univ. of Tokyo, Kashiwa, 277-8582 Chiba

In Collaboration with the members of:
 ICRR, Univ. of Tokyo, Tokyo, Japan; KEK, High Energy Accelerator Organization, Tsukuba, Japan; University of California at Los Angeles, Los Angeles, California, USA; Montana State University, Bozeman MT, USA; Columbia University, Navis Laboratories, Irvington, New York, USA; University of Utah, Salt Lake City, Utah, USA; Kinki University, Osaka, Japan; University of Adelaide, Adelaide, South Australia, Australia;

University of New Mexico, Albuquerque, New Mexico, USA; University of Alabama in Huntsville, Alabama, USA; Yamanashi Univ., Kofu, Japan; Saitama Univ., Urawa, Japan; Konan University, Kobe, Japan; Tokyo Institute of Technology, Tokyo, Japan; Osaka City Univ., Osaka, Japan; Nagasaki Institute of Applied Science, Nagasaki, Japan

Extremely High Energy Cosmic Rays

The origin of the extremely high energy (EHE) cosmic rays is an enigma. Ten events observed by AGASA clearly demonstrate the existence of particles above 10^{20} eV in the universe. As predicted by Greisen Zatsenpin and Kuzmin (GZK), such particles collide with the microwave background and quickly loses its energy by the pion photoproduction. The universe is no longer transparent for EHE particles, and we have to look for the origin of such particles within 50 Mpc (= GZK limit) of our galaxy.

Powerful extragalactic objects such as the active galactic nuclei, radio galaxies and the gamma ray bursts may be suspected as the acceleration site of EHE proton or nucleus. The search for the astronomical origin in the arrival direction of the AGASA events, however, failed to find such objects within 100 Mpc of our galaxy. The origins beyond this limit may be tolerated, but only if we assume special mechanism to allow a longer propagation beyond the GZK cutoff, such as the violation of special relativity or the EHE neutrinos as the carrier of such energy. In addition, it is generally perceived that the astronomical acceleration above 10^{20} eV is difficult to achieve.

It is fascinating to imagine that the EHE cosmic ray is generated by the decay of super-heavy elementary particles in the present universe. The energies above 10^{20} eV are easily obtained if the particle mass is at the Grand Unification scale of 10^{15} GeV. Such particles may be either surviving as a relic particle of the Big Bang or presently generated by the decay of topological defects. An abundant generation of EHE gamma rays and neutrinos, in place of protons and nuclei, is expected in such a decay.

Overview of Experiment

The Telescope Array (TA) experiment is proposed to draw a decisive conclusion on the mysterious origin of EHE cosmic rays[1][2]. It is a giant array of air fluorescence detectors, which measures the UV fluorescence of molecular nitrogen generated by the air shower particles. The observation of the whole shower development process enables an unbiased determination of the energy and arrival direction of incoming cosmic rays. The particle species are determined by measuring the depth of the shower maximum (X_{max}) in the atmosphere. This is the key feature of the experiment.

The effective aperture of TA is more than 30 times larger than that of AGASA. It is approximately the same size as the future ground array experiment, the southern

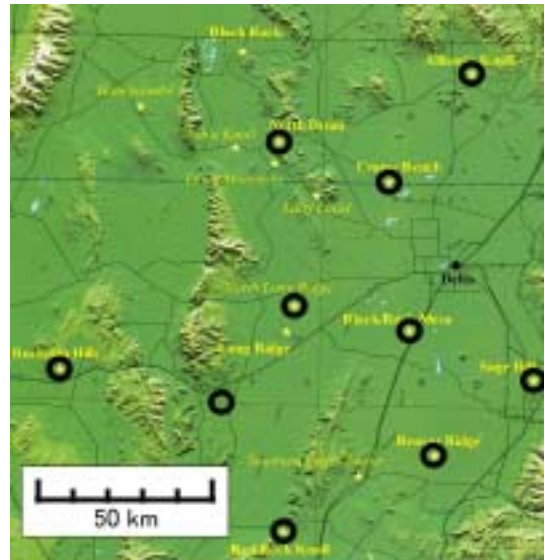


Fig. 1. Proposed station deployment of TA.



Fig. 2. An artist's view of a TA station.

hemisphere Pierre Auger Laboratory, to be constructed in Argentina.

The Telescope Array consists of 10 measurement stations deployed in the West Desert of USA, near Salt Lake City, Utah. Each station is separated by ~ 40 km and is distributed as shown in Fig. 1. Smaller versions of air fluorescence detectors, Fly's Eye and HiRes, have been operating in the vicinity.

Each TA station is equipped with two rings of 20 imaging telescopes arranged in a circle of 30 m diameter (see

Fig. 2). The upper ring covers the elevation angle of 3° – 19° and the lower ring covers 19° – 34° . A total of 40 telescopes covers 360° in azimuth and is sensitive to the cosmic rays above 10^{20} eV falling within 50 km of the station. Most of the cosmic rays will be measured simultaneously by 2 or more stations. This stereo measurement removes an ambiguity of the reconstruction and enables a precise determination of the shower geometry. The development of the shower in the air is recorded by the imaging camera composed of a matrix of photomultipliers (PMTs).

A steerable laser is placed at the center of each station. It will be used to determine the extinction coefficient of the fluorescence light along the transmission path to the telescope.

Telescope

The telescope is composed of a spherical mirror and an imaging camera placed on the focal plane. Eighteen hexagonal segment mirrors form a reflection surface equivalent to a circle of 3 m ϕ with a curvature of radius 6 m . A prototype mirror is shown in Fig. 3. The segment mirror is formed with a 10 mm thick Pyrex glass and an aluminum coating is made by the vacuum deposition. A layer of aluminum oxide is formed by the anodization technique for the protection of the mirror surface.

A set of 256 PMTs with a hexagonal window is arranged in 16×16 array and forms an imaging plane of the camera (see Fig. 4). A single telescope covers the sky of 18° in azimuth and 15.6° in elevation with a pixel ac-



Fig. 3. Prototype mirror.



Fig. 4. Prototype PMT camera.

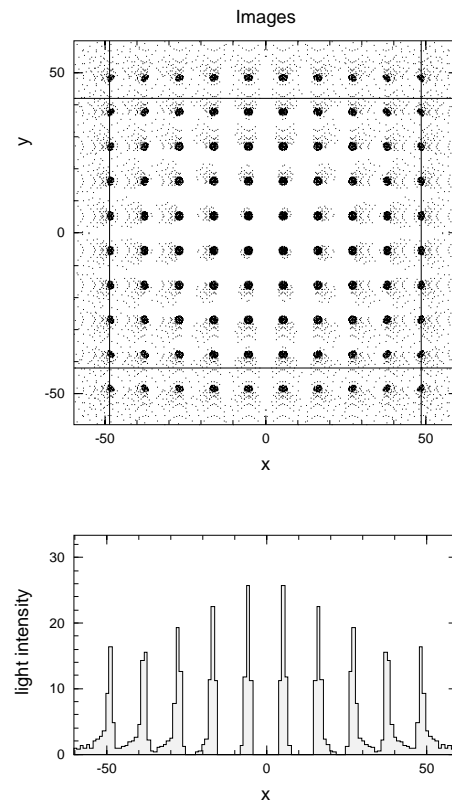


Fig. 5. Optical performance of the telescope. Images formed by parallel lights at different injection angles are shown.

ceptance of $1.1^\circ \times 1.0^\circ$ for one PMT. The image obtained by this optics was simulated by ray tracing and the result is shown in Fig. 5. The average spot size is small enough compared with the size of the PMT photocathode.

The phototube (Hamamatsu R6234 or equivalent) has



Fig. 6. A prototype ADC-DSP board.

a bi-alkali photocathode. A light reflector is placed in the gap between PMTs such that the fluorescence light impinging on the gap is reflected and guided to the central region of the photocathode. This minimizes the insensitive area between PMTs and improves the uniformity of the imaging plane. A UV transparent filter is placed in front of the PMT array to block the night sky background in the visible light region.

An important way of calibrating and monitoring the PMT gain is realized by a small light pulser made by a Cerium activated YAlO_3 scintillator (YAP). An alpha particle from ^{241}Am painted on the scintillator generates $\sim 10^4$ photons around 370 nm, the amount of which can be absolutely calibrated elsewhere. The YAP pulser is mounted on a computer controlled x-y stage in front of the imaging camera. The YAP will scan the PMT imaging plane and the pulse height spectrum of each PMT will be recorded for calibration.

Individual PMTs will be driven by the negative high voltage controlled with an accuracy of 0.1 V. It facilitates the online adjustment of each PMT gain by YAP and opens the possibility of taking data under high background when the Moon is in the sky.

Electronics

A nearby vertical shower produces a PMT signal with short ($\sim 1 \mu\text{s}$) duration but with a high pulse height. A distant shower with a running away configuration produces a long (up to $20 \mu\text{s}$) and weak signal over the night sky background.

The electronics of TA copes with this problem by the combination of custom developed LSI chip (CSI: charge sampling integrator) and a pipeline ADC. It achieves 12-bit resolution, 200 ns sampling time with 16-bit dynamic range by H/L AD conversion scheme. Each readout channel is equipped with a digital signal processor (DSP), which executes a baseline subtraction and signal finding algorithm every $10 \mu\text{s}$. The result is sent to a VME trigger processor by the optical network. The prototype electronics is shown in Fig. 6.

The trigger processor searches for an air shower track in 3-dimensional space XYT ; X and Y being the Cartesian coordinates of the imaging camera and T for the time coordinate. The decision is made within $30 \mu\text{s}$ of the elapsed time and is distributed to each DSP. The DSP makes a data sparcification upon receipt of the trigger,

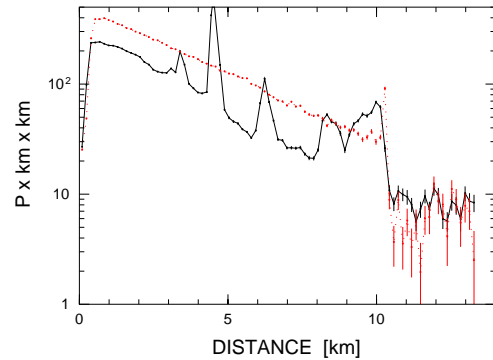
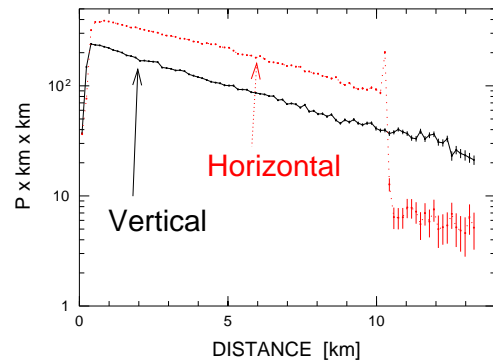


Fig. 7. Attenuation of back scattered light with the distance of transmission for vertical and horizontal laser shots. A good weather (above) and a bad weather (below) examples are shown.

and transport all the data around the discovered shower track for further event building. The ADC and the trigger processor are now installed on the Akeno observatory site together with the prototype telescope, and the integrated system is being tested for the observation of the air shower event.

Atmospheric Monitoring

The fluorescence light undergoes the scattering and absorption before reaching the telescope. The major contribution comes from the molecular (Rayleigh) scattering and the aerosol (Mie) scattering. The strength of Rayleigh scattering can be calculated by using the density profile of the atmosphere. The Mie scattering however depends on the amount and type of the aerosol and its distribution in the atmosphere, which may vary with the place and time.

We plan to install a steerable YAG UV laser system at each station and shoot a laser pulse along the online reconstructed shower track for each event. We measure the side and back scattered laser lights at each station, and derive the extinction coefficient for each event.

We performed such experiments on the HiRes site in Utah and at Akeno observatory in Japan. In the Akeno experiment the laser was shot 256 times at a fixed direction and its back scattered light was measured at the same location (a lidar method)[3]. The strength of the detected signal is shown as a function of the distance to the scattered point in Fig. 7. A similar experiment performed on the HiRes site shows that the attenuation

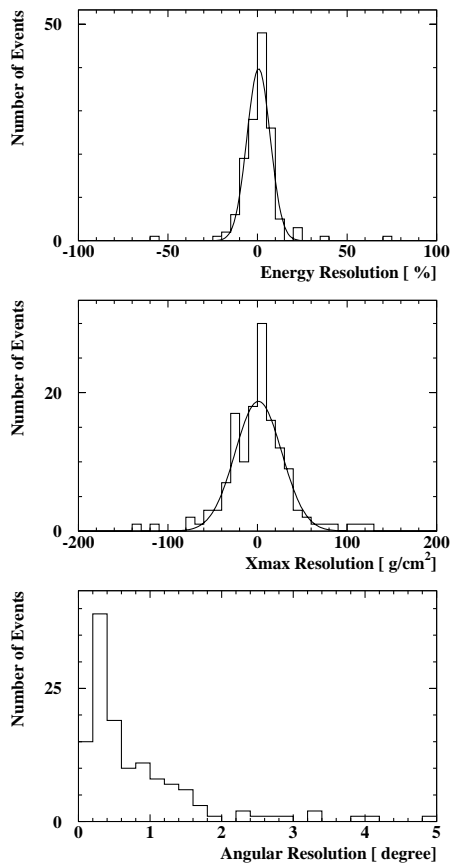


Fig. 8. Reconstruction of energy, X_{max} and arrival direction for 10^{20} eV proton. The resolution of reconstruction is 6%, 25 gr/cm² and 0.6° respectively.

length by the Mie scattering could reach 25 km and is significantly better than the standard atmospheric model of the western US desert [4]. The R/D effort is continuing in Akeno and Utah to obtain a most reliable way of atmospheric correction.

The acceptance of the TA will be reduced by the the cloud obscuring the field of view. We will install a scanning infra-red camera at each station and regularly take a picture of the night sky. The obscuration will also be identified by shooting the laser along the online reconstructed track and observing a large backward scattering.

Performance

The performance of TA for the EHE cosmic rays was estimated by the Monte Carlo study. The longitudinal profile of the air shower was generated by the CORSIKA shower simulation code. The generation, transmission and detection of the fluorescence light was fully simulated. The event was reconstructed from the digitized data by searching for the best arrival direction and shower parameters to fit the observed PMT response including the time profile.

In order to guarantee a reliable stereo reconstruction, we require at least 2 stations have a track extending more than 5° in the field of view. The aperture of the 10^{20} eV

proton with this condition is 64,000 km² sr. We expect to collect more than 30 events of EHE cosmic rays above 10^{20} eV every year with a duty factor of 10%.

The target volume for the EHE neutrino with $E=10^{20}$ eV is 1.1×10^{11} ton sr without considering the duty factor. The detection of HE neutrino is possible by the monocular measurement. The acceptance is 2×10^{10} ton sr for $E=10^{17}$ eV neutrino.

The distributions of the reconstructed energy, X_{max} and arrival direction are shown in Fig. 8 for 10^{20} eV protons. The shape of the reconstructed distribution is well controlled and has no long tails from the average value.

Construction

The Telescope Array will be built by the collaboration of Japanese, American and Australian physicists. The group consists of cosmic ray physicists who have been working in AGASA and HiRes experiments, and high energy physicists who worked in the accelerator experiments in US and Japan.

The development of the mirror, camera and electronics system will be completed in 2002. A prototype telescope will be installed near the planned site in 2003 and its performance will be thoroughly checked.

Bibliography

- [1] The Telescope Array Project: Design Report. July, 2000, available by the web <http://www-ta.icrr.u-tokyo.ac.jp/index.html>.
- [2] T. Aoki et al., Proc. of 27th International Cosmic Ray Conference, 915 (2001).
- [3] T. Yamamoto et al., Proc. of 27th International Cosmic Ray Conference, 663 (2001).
- [4] M. Sasano et al., Proc. of 27th International Cosmic Ray Conference, 653 (2001).

Very High Energy Gamma Ray Observation with Imaging Cherenkov Telescope in Australia: CANGAROO experiment

[Spokesperson : M. Mori]

Air Shower Div., ICRR, Univ. of Tokyo, Kashiwa, Chiba 277-8582

In collaboration with the members of:
 Ibaraki Prefectural University, Ami, Ibaraki;
 Ibaraki University, Mito, Ibaraki;
 Institute of Space and Astronautical Science, Sagami-hara, Kanagawa;
 Konan University, Kobe, Hyogo;
 Kyoto University, Kyoto, Kyoto;
 MSSSO, Australian National University, ACT 2611, Australia;
 National Astronomical Observatory, Mitaka, Tokyo;
 Osaka City University, Osaka, Osaka;
 Shinshu University, Nagano, Nagano;
 STE Laboratory, Nagoya University, Nagoya, Aichi;
 Tokai University, Hiratsuka, Kanagawa;
 Tokyo Institute for Technology, Meguro-ku, Tokyo;

University of Adelaide, Adelaide, SA 5005, Australia;
 Yamanashi Gakuin University, Kofu, Yamanashi;
 Yamagata University, Yamagata, Yamagata.

Very high energy (VHE) gamma-rays at TeV energies are searched for in the southern sky by the CANGAROO Collaboration as an international collaboration with Australian universities. The new imaging Cherenkov telescope (CANGAROO-II), first built with a 7-m diameter reflector in 1999, was expanded to have a 10-m reflector, in February 2000 in Woomera, South Australia, ($136^{\circ} 47' E$, $31^{\circ} 06' S$), and has been in operation on moonless, clear nights. The optical reflector is composed of 114 spherical mirrors of 80 cm in diameter made of composite material (mainly CFRP) arranged to form a parabolic surface and has a focal length of 8 m [1]. A multi-pixel photomultiplier-tube camera is set at the focal plane, giving a field of view of $2.76^{\circ} \times 2.76^{\circ}$. Each pixel of photomultiplier tube views $0.115^{\circ} \times 0.115^{\circ}$. The outputs of the photomultiplier tubes are digitized and used to reconstruct the image of Cherenkov light emitted from air shower particles created by very high energy γ -rays (sub-TeV in energy) in the upper atmosphere. The arrival direction of γ -rays is determined with an accuracy of $\sim 0.2^{\circ}$ as well as to distinguish from Cherenkov light images of cosmic-ray background events.

With the 10-m telescope, we have observed various objects which includes gamma-ray sources we have detected with the 3.8-m telescope, CANGAROO-I: the Crab pulsar/nebula, the pulsar PSR 1706-44, supernova remnants SN1006 and RX J1713.7-3946, and the pulsar PSR 1509-58. We also observed other candidate objects such as active galactic nuclei (AGN). The results are summarized in the following sections.

Now we are constructing an array of four 10-m Cherenkov telescopes, called CANGAROO-III, which will be completed by 2003 [2]. With its stereoscopic imaging capability of Cherenkov light, we will explore the high energy universe with excellent sensitivities [3]. In March 2002 the second 10-m telescope was constructed 100-m west of the first telescope (Fig. 9). It is equipped with an improved multi-pixel camera which has a wider field-of-view of 4 degrees [4], refined mirrors and faster electronics. This telescope is under tuning to commence stereoscopic observation of Cherenkov light which enables us to detect gamma-rays with higher resolution.

PSR 1706-44 and SN1006

These sources are extensively studied by Kyoto University group. The preliminary results are obtained and presented at 27th ICRC in Aug. 2001 [5, 6, 7]. Both sources were re-confirmed to be there. The fluxes are consistent with the previous measurement with CANGAROO-I. For detail, one can see the above references.

RX J1713.7-3946: one of cosmic ray origin?

With the 10-m telescope, we have confirmed RX J1713.7-3946 as a TeV source [8, 9]. The image orientation angle (α) is plotted in Fig. 10 (the inserted graph). The α distribution is broad as if it is a diffuse



Fig. 9. The second 10-m telescope completed in March 2002. The first telescope can be seen in the background.

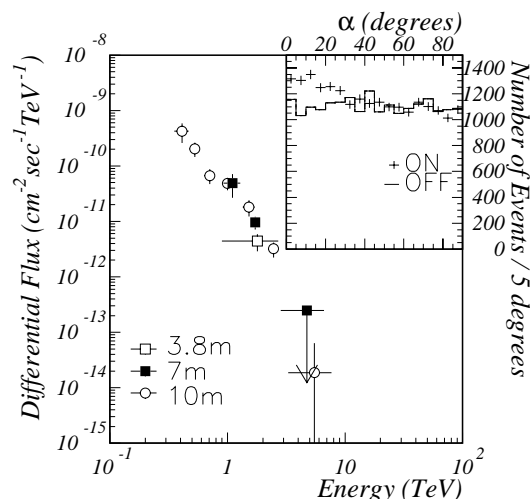


Fig. 10. Differential flux of RX J1713.7-3946 obtained by CANGAROO-II. The white circles are obtained by the 10-m telescope, black squares are by the 7-m, and white squares are by the 3.8-m. The inserted graphs are image orientation angle α for ON- (points with error bars) and OFF-source run (histogram).

source, consistent with the previously published result [10]. The statistical significance of the α -peak is 8.7σ . Also the differential flux is obtained as shown in Fig. 10, consistent with ref. [10]. The power law spectrum is observed even in the sub-TeV region which is extended to less than 400 GeV, whose behavior is hard to understand if the emission is produced by high-energy electrons via inverse Compton or bremsstrahlung processes. Instead, the emission is consistent with gamma-rays produced via decay of neutral pions emitted in collisions of high-energy protons with surrounding matter of this SNR. This can be an evidence that this SNR is one of birth places of cosmic-ray protons and cast a prospect of the long-standing problem of cosmic-ray origin [11].

Southern AGNs

The analysis of southern nearby AGNs are carried out

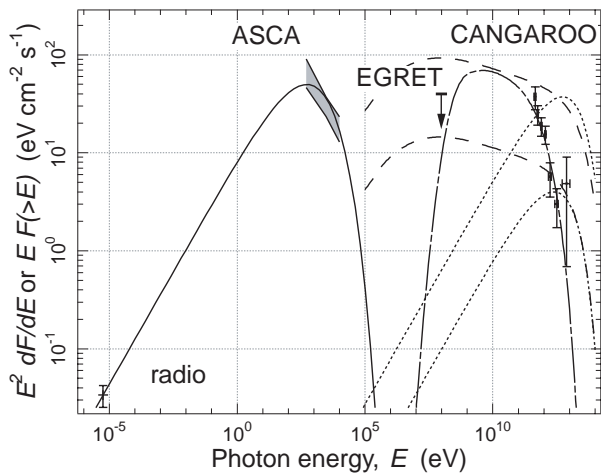


Fig. 11. Multiwavelength spectrum of RX J1713.7-3946 and emission models. Lines show model calculations: synchrotron emission (solid line), inverse Compton emission (dotted lines), bremsstrahlung (dashed lines) and emission from neutral pion decay (short-long dashed line). Inverse Compton emission and bremsstrahlung are plotted for two cases: $3 \mu\text{G}$ (upper curves) and $10 \mu\text{G}$ (lower curves). See ref. [9] for details.

by Tokai University group. The preliminary results based on observations of PKS 2155–304 and PKS 2005–489 in 2000 were presented at 27th ICRC [12]. We could not see gamma-ray signals from both sources and obtained upper limits which are lower than some of theoretical predictions. We are promising that we can carry out a systematic study on the mechanism of cosmic-ray emission from AGN jets.

Mrk 421 observed at large zenith angles: question on cosmology

We observed Mrk421, a nearby AGN and an established TeV gamma-ray source in the northern hemisphere, in Jan. to Feb. 2001 when it was in high state. The zenith angles for this observation was around 70 degrees. The trial for such a large zenith angle observation was a challenge to the atmospheric Cherenkov method. Due to the slant depth of atmosphere, the energy threshold becomes as high as 10 TeV, but the detection area becomes wider and we have sensitivities to low gamma-ray fluxes. Analysis of the data shows a gamma-ray signal of which significance is greater than 5σ [13, 14]. TeV photons collide with infrared photons and produce electron-positron pairs. The mean free path of this absorption becomes important for cosmological distances. In the case of Mrk421 ($z = 0.03$), previous estimate of intergalactic infrared background flux predicts a cut-off in energy spectrum of around several TeV. The detection of over 10 TeV photons is not compatible with such estimate and may require reassessment of background photon flux in the Universe.

NGC 253: completely new window

NGC 253 is one of the closest starburst galaxies. High star formation rate means copious supernova remnants and could be a new category of TeV gamma-ray sources.

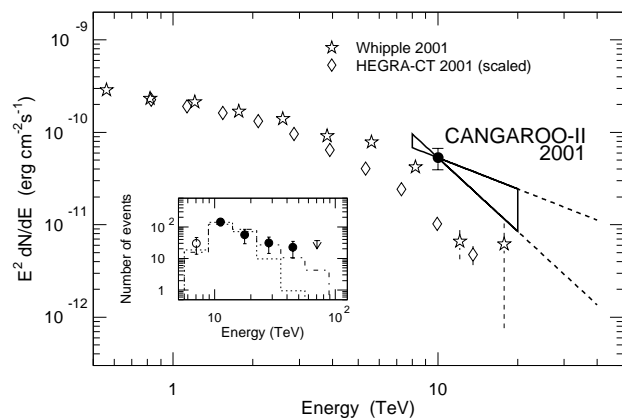


Fig. 12. The observed gamma-ray (main panel) and the energy spectrum of gamma-ray events (inserted panel). In the inserted panel, data are represented by circles with error bars, with a 2σ upper limit plotted at the highest energy. Best-fit spectra for a power-law ($E^{-4.0}$; dot-dashed line) and a cut-off ($E^{-1.9} \exp(-E/4 \text{ TeV})$; dotted line) are shown. See ref. [14] for details.

It can be seen from the southern hemisphere with a good condition, i.e., it culminates near zenith. The observation was carried out in Oct. 2000 and Oct. 2001. Gamma-ray signals were detected in both the data obtained in 2000 and 2001. The flux is very faint, such as several times weaker than the Crab nebula. Ibaraki university and ICRR group have completed the analysis and a paper has been submitted for publication [15].

Other targets

A supernova remnant RCW 86 and a pulsar PSR 1259–63 have been observed in Mar. 2001. The analyses are underway by Kyoto group (RCW 86) and ICRR (PSR 1259–63). Other targets, such as the Galactic center, SS443, and RX J0852–4622 were observed in 2001 and analyses are underway.

Near future prospect

The tuning of the second 10-m telescope will be completed in November 2002 and stereoscopic observation of Cherenkov images will begin with two 10-m telescopes. The complete array of four telescopes will be completed by 2003. Even considering the schedule of the HESS project in Namibia, we are still ahead. The efforts in the first one or two year are very important to us.

Summary

This year has been very productive, we think, and many interesting results are coming out as described above. With improved sensitivity of stereo imaging technique, we hope our understanding of the high-energy universe will be put forward.

Bibliography

- [1] A. Kawachi et al., *Astropart. Phys.*, **14**, 261–269 (2001).
- [2] M. Mori et al., *AIP Conference Proceedings* 587, pp. 927–931 (2001); *Proc. 27th ICRC (2001) Vol.5*, pp. 2831–2834.
- [3] R. Enomoto et al., *Astropart. Phys.*, **16**, 235–244 (2002).
- [4] S. Kabuki et al., *Nucl. Inst. Meth. Phys. Res. A* (in press).
- [5] J. Kushida et al., *Proc. 27th ICRC (2001) Vol.6*, pp. 2424–2427.
- [6] T. Tanimori et al., *Proc. 27th ICRC (2001) Vol.6*, pp. 2465–2468.
- [7] S. Hara et al., *Proc. 27th ICRC (2001) Vol.5*, pp. 2455–58.
- [8] R. Enomoto et al., *Proc. 27th ICRC (2001) Vol.5*, pp. 2477–2480 .
- [9] R. Enomoto et al., *Nature*, **416**, 823–826 (2002).
- [10] H. Muraishi et al., *Astron. Astrophys.*, **354**, L57–61 (2000).
- [11] F. Aharonian, *Nature*, **416**, 797–798 (2002).
- [12] K. Nishijima et al., *Proc. 27th ICRC (2001) Vol.5*, pp. 2626–2629.
- [13] K. Okumura et al., *Proc. 27th ICRC (2001) Vol.5*, pp. 2679–2682.
- [14] K. Okumura et al., *Astrophys. J. Lett.* (in press).
- [15] C. Itoh et al., submitted for publication.

EMULSION DIVISION

Overview

The Naming of the Emulsion Division was historically by the group activities of the early days, the present division covers the fields of research activities much wider than the name may suggest. It consists of two main groups, one is the experiment group and the other is the theory group. The former aims to clarify high-energy cosmic ray interactions and primary cosmic ray composition in high-energy region, mainly by means of emulsion or related technique. The latter carries out the theoretical research of astro-particle physics in general.

A large-area emulsion-chamber experiment started in the early 197's, being successively carried out at the top of Mt. Fuji (at 3 750 m a.s.l.) in order to study the properties of high-energy hadron interactions as well as the chemical composition of cosmic rays around 10^{15} – 10^{17} eV, came to an end with a great success in 1994. Emulsion chambers were often taken on board balloons at the Sanriku Balloon Center of ISAS in order to obtain direct information on cosmic ray composition as well as high energy heavy-ion interactions at energies around 10^{13} – 10^{14} eV. New results on the heavy primary spectrum from ~ 100 GeV/particle to ~ 100 TeV/particle were obtained by the Hirosaki-Aoyama Gakuin group. The chamber uses a multi-layered sandwich of X-ray films (SXF), nuclear emulsion plates and target layers. An auto-scanning system was developed to identify interaction vertices for this experiment.

International collaboration plays an important role in the activities of this division. A large-scale emulsion chamber project was carried out with Chinese physicists at Mt. Kanbala (5 500 m a.s.l.) in Tibet during the period from 1980 through 1990, with fruitful results. The same project, however, is still being conducted with Brazilian physicists at Mt. Chacaltaya (5 200 m a.s.l.) in Bolivia. These large-scale emulsion chambers can directly observe the phenomena induced by primary cosmic rays of 10^{15} – 10^{17} eV. Some interesting results are briefly reported below.

An air shower experiment aiming to search for celestial gamma-ray point sources started in 1990 with Chinese physicists at Yangbajing (Tibet, 4 300 m a.s.l.) and has been successful. An extension of the air shower array was completed in 1995 and an emulsion chamber has been combined with this air shower array since 1996 to study the primary cosmic rays around the knee energy region. The Tibet air shower array has a good angular resolution better than 1 degree for air showers even at multi-TeV energy region, with the result that the solar magnetic field effect on the cosmic ray shadow by the sun was for the first time observed in 1992. From this experiment with better statistics, new information is expected to be obtained on the large-scale structure of the solar and interplanetary magnetic field and its time variation

due to the solar activity cycle.

Balloon borne emulsion-chamber experiments have been carried out with US physicists at Texas in the U. S. or in the Southern Hemisphere from Australia to Brazil in order to achieve a long-duration exposure flight. In December of 1993 the antarctic balloon loaded emulsion chambers were launched from MucMuro base (78°S) and successfully recovered after 200 hours. The energy spectra of protons, helium nuclei and others have been obtained up to about 10^{14} eV, and helium nuclei show a slightly flatter spectrum than protons at high energies.

The JANZOS (Japan Australia New Zealand Observation of Supernova) project, being successfully carried out at Black Birch Range since 1987, was completely finished in March of 1995. The results obtained by this experiment have already been published in many scientific journals.

A theory group has been added to this division since 1979. The group is working on astro-particle physics, including cosmology, super-symmetry phenomenology, and baryo-genesis. Though the group is small, it has been active and published about 60 papers in refereed journals during last 5 years.

The development of various detectors for new experiment is being made by introducing new technology such as scintillating fiber, super-conducting magnet etc. A superconducting solenoid spectrometer was completed in 1993 to use for cosmic-ray balloon experiments in 1995. A scintillating fiber calorimeter has been developed to use for the observation of GeV gamma rays on board satellites in future.

This division has developed and completed several automatic measuring systems that are powerful for analyzing cosmic ray tracks or shower spots, that is, automatic microdensitometers and precise coordinate-measuring systems controlled by a computer. Enormous data recorded on nuclear emulsion plates or X-ray films are rapidly and precisely measured by the use of these measuring systems. At present five workstations are introduced to improve data-processing capacity.

The division's emulsion-pouring facilities can meet the demands for making any kind of nuclear emulsion plates which are used for cosmic ray or accelerator experiments. The thermostatic processing facilities are favorably operated in order to develop nuclear emulsion plates or X-ray films. Using these facilities, it is also possible to make and develop emulsion pelicles of 600 micron thickness each. In this way these facilities are made available to all qualified scientists who want to carry out joint research successfully.

Search for Celestial Gamma-Ray Point Sources and Study of Cosmic-Ray Composition at the “Knee” Energy Region in the Tibetan Highlands (The Tibet AS γ Collaboration)

[Spokesperson : Masato Takita]

ICRR, Univ. of Tokyo, Kashiwa, Chiba 277-8582

In collaboration with the members of:

Hirosaki Univ., Hirosaki; Utsunomiya Univ., Utsunomiya; Saitama Univ., Urawa; Kanagawa Univ., Yokohama; Yokohama National Univ., Yokohama; Shonan Inst. of Technology, Fujisawa; Tokyo Metropolitan Coll. of Aeronautical Eng., Tokyo; NACSIS, Monbusho, Tokyo; Konan Univ., Kobe, Waseda Univ., Tokyo, Shibaura Inst. of Technology, Tokyo, Nagoya Univ.; China

Since 1990 the Tibet air shower array has been successively operated at Yangbajing (4 300 m above sea level) in Tibet. Some results obtained from this experiment have been reported elsewhere. The air shower array (Tibet-I) was updated in late 1994 by increasing the number of scintillation detectors from 65 to 221, and then this new array (called as Tibet-II) has been fully operating. The Tibet-II array consists of 185 first-timing (FT) detectors of 0.5 m² each. For the FT detectors, plastic scintillators of 3 cm thickness each are used and 2'' ϕ PMTs (HPK H1161) are equipped. They are placed in a grid of a 15 m spacing, as the previous array. Among these, each of 52 FT detectors also contains a 1.5'' ϕ PMT (HPK H3178) for a wide-range particle density measurement. The FT array is also surrounded by 32 density detectors of 0.5 m² each to obtain a good core location for individual shower event. The effective area for detecting the contained events is about 8 times as large as the old one, and shower events has been accumulated at a rate of about 150 Hz to efficiently detect showers with energies around 10 TeV. In 1996, a dense array was constructed near the center of the Tibet-II array. This array (HD-array) consists of 110 scintillation detectors each being placed at a grid of 7.5 m spacing and was sensitive to air showers with energies around 3 TeV. A trigger rate of this array has been set to about 150 Hz. Using this HD array, in 1999, we succeeded in observing γ -ray signals from the Crab Nebula at 5.5 σ confidence level. This was the first detection of multi-TeV γ -ray signals by a conventional air shower array. Following it, we also detected multi-TeV γ -rays successfully at 3.7 σ level from Mrk501 which was in a highly flaring state between March 1997 and August 1997.

In the late fall of 1999, the area of the HD array was enlarged up to 22000 m² (Tibet-III) as shown in Fig. 1. It is equipped with 533 scintillation counters (497 FT + 36 density PMTs) in total. The trigger rate is 680 Hz.

The performance of the array has been well examined by observing the Moon's shadow, and the deficit map of cosmic rays around the Moon gives an angular reso-



Fig. 1. Tibet-III array operating at Yangbajing.

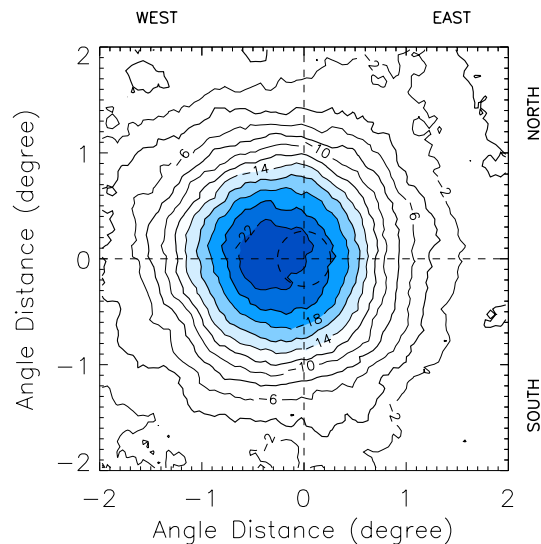


Fig. 2. Moon shadow observed by Tibet-III.

lution of the array to be around 1.0° for the Tibet-III array, as is shown in Fig. 2. Multi-TeV gamma-ray signal was successfully detected at $\sim 5\sigma$ level from the Crab (the standard candle in gamma-ray astronomy) by the Tibet-III array, as shown in Fig. 3. We also succeeded in observing multi-TeV gamma-ray flares at $\sim 7\sigma$ level from Markarian 421 which was in a very active phase during the year 2000 and 2001, shown in Fig. 4. We are now accumulating Tibet-III data to obtain a standard TeV γ -ray flux and to search for unknown constant/transient TeV γ -ray sources.

A hybrid experiment of emulsion chamber (EC) and air shower array started in 1996 to obtain the proton flux around the knee of the primary cosmic ray spectrum. The total area of EC each having the size of 40 cm \times 50 cm is 80 m² and the total thickness of lead plates is 14 r.l. High sensitive X-ray films are inserted at every 2 r.l. to detect gamma-ray families. Just under the emulsion chambers, the burst detectors with the same area as EC were set up to locate the shower cores of family events to be observed in the emulsion chambers. This detector complex is set up near the center of the Tibet-II array to get on the information about accompanying air showers. The first EC exposure was terminated in August

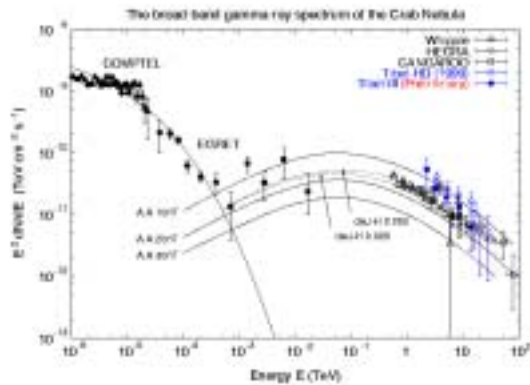


Fig. 3. Energy spectrum of gamma rays from the Crab observed by Tibet-III.

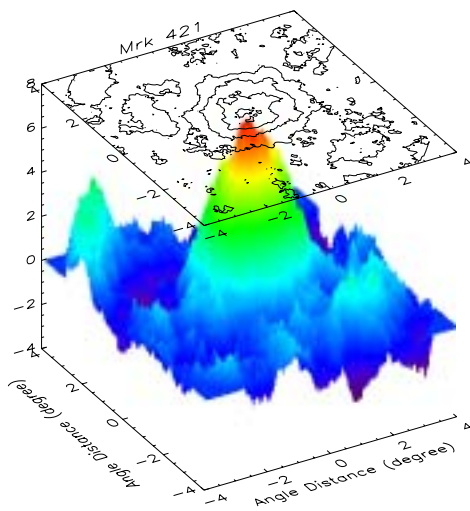


Fig. 4. Gamma-ray signal around Mrk421 in its flaring phase in the year 2000 and 2001 observed by Tibet-III.

of 1997 and X-ray films inserted in EC were developed for analysis. Many gamma-ray families were detected in the EC and a correspondence between these families and their accompanied air showers is now in progress by using the data from burst detectors, emulsion chambers and air shower array. A high-energy family event of about 500 TeV was observed in this exposure and its primary energy is estimated to be about 10^{16} eV from the size of accompanying AS. This hybrid experiment continued until 1999. Using the burst + air shower array data, we obtained the energy spectrum of primary protons (820 proton-induced events during 690-day detector live time) with its primary energies 200–1000 TeV by a neural network method. The differential energy spectrum obtained in this energy range can be fit by a power law with the spectral index of -2.97 ± 0.06 , which is steeper than that obtained by direct measurements at lower energies. We also obtained the energy spectrum of helium nuclei. All of the features of burst events are wholly compatible the heavy enriched composition in the knee region. The pri-

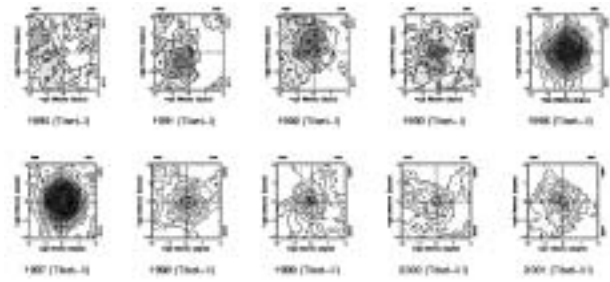


Fig. 5. Yearly variation of the Sun's shadow observed by the Tibet-I (1991, 1992), Tibet-II (1996, 1997, 1998, 1999) and Tibet-III (2000, 2001) arrays, respectively. Mode energies are 10 TeV.

mary proton spectrum including the EC data around the knee region, being inaccessible by any direct observations, are being analyzed. Roughly one third of the EC data has been analyzed. Automatic analysis programs are under development.

As discussed elsewhere, this array will be very powerful to get new information on the relation between a time variation of the large structure of the solar and interplanetary magnetic fields and the solar activity, since sufficient data taken from this array can follow the movement of the sun shadow at every one-two months. The sun's shadow was observed in the direction significantly away from the apparent sun's position during the period from 1990 through 1993. Note that this period almost corresponds to the solar cycle near the maximum or at the decreasing phase (Cycle 22). In 1996 and 1997, however, we found that the sun's shadow was observed almost at the same position as the Sun, since the solar cycle is now in a quiet phase. Since 1998, the sun's shadow began to be obscure shown in Fig. 5, as the solar activities restarted. We expect that the Sun's shadow will change again its position according to the solar activity as the next solar cycle (Cycle 23) goes toward its maximum around the year of 2001. Thus, the results will considerably contribute to the study of solar terrestrial physics.

Exotic Phenomena Observed by Mountain Emulsion Chamber (Chacaltaya Collaboration)

[Spokesperson: Akinori Ohsawa]

ICRR, Univ. of Tokyo, Kashiwa, Chiba 277-8582

In collaboration with the members of: Waseda Univ., Tokyo; Aoyama Gakuin Univ., Tokyo; Yamanashi Univ., Kofu; Saitama Univ., Urawa; Kochi Univ., Kochi; Kinki Univ., Osaka; USSR; Brazil

A series of emulsion chamber exposures have been continuously carried out at Mt. Chacaltaya (5300 m) since 1963. Several interesting events including Centauro-type events have been observed in the emulsion chambers with carbon target layer so far exposed at the Chacaltaya Observatory by Chacaltaya group of Brazil-Japan Collab-

oration and Pamir-type chamber exposed at the Pamir station (4 300 m) in collaboration with the Pamir group. Details of these events were already published elsewhere.

An over-all interpretation of exotic cosmic-ray phenomena is under study. A possible scenario is examined under the hypothesis of the existence of quark matter. The core of a compact star can be made of quark matter with u,d and s quarks, which is more stable, under high pressure than ordinary nuclear matter. Violent stellar activity has a chance of emitting the core material into outer space, and a small globule of the quark matter would be positively charged and accelerated to the cosmic-ray energy region. When such quark-matter globule comes into the atmosphere, it undergoes nuclear interactions with characteristics that are different from the common nuclear interactions. The incoming globule is made of a small dense core with high baryon number and the surrounding pion cloud. A core collision results in multiple baryon production, like the Centauro-type, and fragmentation of the quark-matter globule. Here, one expects emission of an excited quark-globule, which can then transition into a bundle of hadrons and electromagnetic particles.

A new project (OMEGA) is worked out to study hadronic interactions at energies around 10^{15} – 10^{17} eV by constructing a large-scale emulsion chamber combined with an air shower array at Mt. Chacaltaya. The air shower array provides information on the primary cosmic-ray energy and the stage of air shower development at the observation level. A clue to solving the anomalous behavior of families mentioned above is expected to be given by such hybrid experiment. A small-scale experiment has been continued at Mt. Chacaltaya and some results were reported elsewhere.

Theory Group

Time Evolution of Tunneling Phenomena

[Spokesperson at ICRR: M. Yoshimura]

ICRR, Kashiwa 277-8582

Collaboration with the members of ICRR

Matsumoto and Yoshimura studied time evolution of tunneling phenomena occurring in thermal medium. The time-dependent tunneling rate and the survival probability were derived by using the real-time formalism. The effect of environment, especially its influence on the time evolution was clarified in this work. It was found that a nonlinear resonance effect enhances the tunneling rate at finite times of order $2/\eta$, with η the friction coefficient. In the linear approximation this effect has relevance to the parametric resonance. This effect is expected to enhance the possibility of early termination of the cosmological phase transition much prior to the typical Hubble time.

References

[1] Sh. Matsumoto, Soryushiron Kenkyu (Kyoto) 104 (2002), B21.

Primordial magnetic field generation in cosmological phase transitions

[Spokesperson at ICRR: T. Uesugi]

ICRR, Kashiwa 277-8582

The existence of coherent magnetic fields over various astrophysical scales has been established up to the present. To explain the observed magnetic field in galaxies, clusters, and interclusters, we studied a generation of the seeds of primordial magnetic fields during cosmological phase transitions. In the previous study, we estimated the primordial magnetic field generated by gauged Q-balls during the electroweak phase transition. At the electroweak scale, however, coherent scale of the generated magnetic field cannot become larger than galactic scales. To explain the large scale magnetic field, we are considering the generation mechanism due to a non-equilibrium process during inflationary universe.

Delocalization Transition and Localization Length of Random Mass Fermions in an Imaginary Vector Potential

[Spokesperson at ICRR: K. Takeda]

ICRR, Kashiwa 277-8582

Collaboration with the member of Nagoya Institute of Technology

It is believed that almost all states tend to localize in disorder systems in two and lower dimensions. However, it was shown by the recent studies that some specific states remain extended in the presence of correlated disorder. We studied one-dimensional system of Dirac fermions with a random-varying mass by the transfer-matrix method which we developed recently [1]. We investigated the effects of nonlocal correlation of the spatial-varying Dirac mass on the delocalization transition. In particular, we calculated both “typical” and “mean” localization lengths as functions of energy, using imaginary vector potential. The results of numerical study are in good agreement with the ones of analytical calculations. We also obtained the relation between the localization length of states and the correlation length of the random mass.

References

[1] K. Takeda and I. Ichinose, J. Phys. Soc. Jpn. 70 p3623 (2001).

Study on AdS/CFT and dS/CFT Correspondence

[Spokesperson at ICRR: N. Yokoi]

ICRR, Kashiwa 277-8582

Collaboration with the members of Osaka Univ., Ibaraki Univ., and KEK

The AdS/CFT correspondence is the correspondence between supergravity or superstring theory on the Anti-de Sitter (AdS) space-time and the superconformal field

theory (CFT) on its boundary. We studied the quantum corrections for the supergravity on the AdS background and an extension of the holographic renormalization group in order to investigate the AdS/CFT correspondence at the sub-leading order of $1/N$ expansion of the CFT [1]. We also studied the quantum aspects of the three-dimensional gravity with a positive cosmological constant from the perspective of the dS/CFT correspondence, which is the correspondence between quantum gravity on de Sitter space-time and a certain CFT [2].

References

- [1] T. Kubota, T. Ueno and N. Yokoi, in preparation.
 [2] H. Umetsu and N. Yokoi, in preparation.

List of Other Inter-University Research Programs

Code No.: 6

Title: Study of primary cosmic rays by RUNJOB

Spokesperson: T. Shibata (Aoyama Gakuin University)

Participating Institutions: Aoyama Gakuin Univ., Hiroshaki Univ. and

Shonan Institute for Technology, Gifu Univ.

Code No.: 7

Title: Observation of High-Energy Electrons and Gamma Rays with a Balloon-borne Instrument

Spokesperson: Shouji Torii (Kanagawa University)

Participating Institutions: Kanagawa Univ., ISAS, Rikkyo Univ.,

ICRR Univ. of Tokyo, and Shibaura Inst. of Technology.

Code No.: 8

Title: Observation of high-energy primary electrons and atmospheric gamma rays by emulsion chambers.

Spokesperson: T. Kobayashi (Aoyama Gakuin University)

Participating Institutions: Utsunomiya Univ., Kanagawa Univ., ICRR Univ. of Tokyo, Univ. of Tokyo, Kanagawa Prefectural College of Nursing and Medical Technology.

Code No.: 9

Title: Sidereal daily variation of 10 TeV-region galactic cosmic-ray intensity observed by the Tibet air shower array .

Spokesperson: K. Munakata (Shinshu University)

Participating Institutions: Shinshu Univ.

RESEARCH CENTER FOR COSMIC NEUTRINOS

Research Center for Cosmic Neutrinos was established in April 1999. The main objective of this center is to study neutrinos based on data from various observations and experiments. In order to promote the studies of neutrino physics, it is important to provide the place for discussions on theoretical ideas and experimental results on neutrino physics. Therefore, one of the most important, practical jobs of this center is the organization of neutrino related meetings.

In the fiscal year 2001, we organized three local neutrino meetings. Two of them were held in ICRR, and one in Tokyo Metropolitan University. In these meetings, we have discussed topics such as, atmospheric neutrinos, solar neutrinos, supernova neutrinos, accelerator neutrino experiments, reactor neutrino experiments, double beta decay, phenomenology of neutrino oscillations, CP violation in neutrino sector, models of neutrino mass, and unified theories. In each meeting, we had about 50 participants.

Atmospheric neutrino data from Super-Kamiokande give the most precise information on neutrino oscillations. With the increased data, it is more important to have better predictions of the neutrino flux. Therefore, we work on the prediction of the atmospheric neutrino flux. In order to predict the flux accurately, it is

important to know the details of the data on the measurements of primary and secondary cosmic ray fluxes. For this reason, we have a close collaboration with researchers working in the cosmic ray flux measurements. The preliminary results from the new detailed calculation shows about 10% smaller absolute flux than the previously used flux. Also, the new flux, which is calculated including the accurate three dimensional geometry of the Earth and the interaction, shows an enhancement of the flux in the horizontal direction for sub-GeV neutrinos.

It is important that the general public knows the achievements of the present science. Because of this reason, we had a public lecture at Kashiwa, the city our new campus is located. Three active scientists related to neutrino physics lectured on various aspects of neutrino physics.

Finally, scientific staffs in this center are actively working in the Super-Kamiokande and K2K experiments.

OBSERVATORIES and STATIONS

Location of the Institute and the Observatories in Japan

OBSERVATORIES and STATIONS

Norikura Observatory

Location: Nyukawa-mura, Ohno-gun, Gifu Prefecture 506-2100
N 36°06', E 137°33', 2770 m a.s.l.
Telephone (Fax): +263-33-7456
Telephone (satellite): 090-7721-5674
Telephone (car): 090-7408-6224

Akeno Observatory

Location: Akeno-mura, Kitakoma-gun, Yamanashi Prefecture 407-0201
N 35°47', E 138°30', 900 m a.s.l.
Telephone: +551-25-2301
Fax: +551-25-2303

Kamioka Underground Observatory

Location: Higashi-mozumi456, Kamioka-cho, Yoshiki-gun, Gifu Prefecture 506-1205
N 36°25'26", E 137°19'11", 357.5 m a.s.l.
Telephone: +578-5-2116
Fax: +578-5-2121

See Kamioka Division for the research activities.

NORIKURA OBSERVATORY

Norikura Observatory (36.10°N and 137.55°E) was founded in 1953 and attached to ICRR in 1976. It is located at 2770 m above sea level, and is the highest altitude manned laboratory in Japan maintained all the year. Experimental facilities of the laboratory are made available to all the qualified scientists in the field of cosmic ray research and associated subjects. The AC electric power is generated by the dynamo and supplied throughout the observatory. In 1996, two dynamos of 70 KVA each were replaced with the new ones. The observatory can be accessed easily by the car in summer (June-October) but an aid of snowmobile is necessary in winter time.



Fig. 1. Norikura Observatory.

Present academic interests of the laboratory is focused on the modulation of high energy cosmic rays in the interplanetary space associated with the solar activity and the generation of energetic particles by the solar flares.

For the modulation study, two small experiments have been operated continuously for a long time. One is a neutron monitor operated to study the correlation of solar activity and the cosmic ray flux. The other is a high counting meson telescope consisting of 36 m² scintillation counters to study the time variation of cosmic rays with energies of 10–100 TeV.

The Sun is the nearest site to the Earth capable of accelerating particles up to high energies. When the Sun becomes active, flares are frequently observed on its surface. The flare accelerates the proton and ion to high energy and they are detected on the Earth soon after the flare. Among the particles generated by the flare, high energy neutrons provide the most direct information about the acceleration mechanism as they come straight from the flare position to the Earth without being affected by the magnetic field.

The detection of solar flare particles has been very active in the Norikura observatory for the last 10 years. The muon telescope of the observatory successfully detected

flare particles in association with a large flare occurred on the 29th of September, 1989. The data suggested that protons could be accelerated at least up to 50 GeV in a large solar flare considering the geomagnetic cut-off rigidity of the proton is estimated to be 11.5 GeV at Mt. Norikura. The high altitude of the observatory is essential for detecting the flare particles without significant attenuation.

In 1990, Nagoya group constructed a solar neutron telescope consisting of scintillators and lead plates, which measures the kinetic energies of incoming neutrons up to several hundred MeV. This telescope observed high energy neutrons associated with a large flare occurred on the 4th of June, 1991. The same event was simultaneously detected by the neutron monitor and the high counting meson telescope of the Norikura observatory. This is the most clear observation of solar neutrons at the ground level in almost ten years since the first observation at Jungfrauoch in 1982.

A new type of large solar neutron telescope (64 m² sensitive area) was constructed by Nagoya group in 1996. It consists of scintillators, proportional counters and wood absorbers piled up alternately. This takes a pivotal role among a worldwide network of ground based solar neutron telescopes of the same type in Yangbajing in Tibet, Aragatz in Armenia, Gornergrat in Switzerland, Chacaltaya in Bolivia and Mauna Kea in Hawaii. The Sun is being watched for 24 hours using this network.

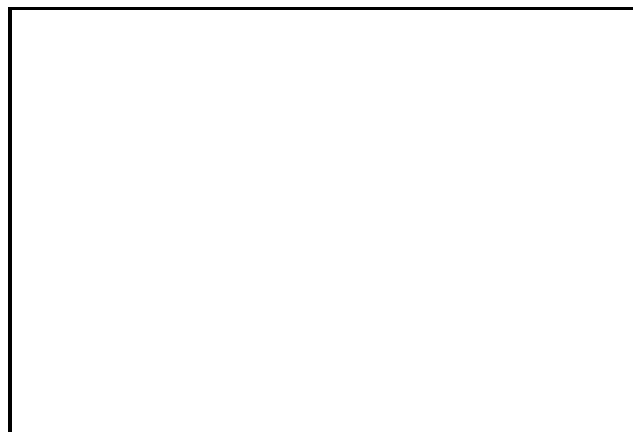


Fig. 2. New Solar-Neutron Telescope of Nagoya Group.

The Sun is reaching the maximum activity in 2001 and the active phase will continue for next few years. All the telescopes in the Norikura observatory, neutron, meson and muon telescopes, will be operated continuously through this solar cycle (Cycle 23) in order to obtain comprehensive information on the solar flare phenomena. Important hints for understanding the mechanism of cosmic ray acceleration will be obtained by this measurement.

In addition to the long-term cosmic-ray observations mentioned above, various kinds of short-dated experiments are carried out every year taking an advantage of the high altitude of the observatory. As a few examples, following experiments have been performed; a search for super heavy particles with plastic plates, a precise measurement of atmospheric gamma rays and muons, collection of cosmic dusts contained in the snow and the performance study of the balloon borne cosmic ray experiments. A part of the facility has been open for the environmental study at high altitude such as the aerosol removal mechanism in the atmosphere.

AKENO OBSERVATORY

The Akeno Observatory has evolved into a complex scientific center for studying ultra-high-energy cosmic rays through extensive air showers in the energy range 10^{15} eV \sim 10^{20} eV, and is being used by many universities. The Observatory is in Akeno village, located about 20 km west of Kofu-city and about 130 km west of central Tokyo. Its altitude is 900 m above sea level, and the location is at longitude 138.5°E and latitude 35.5°N . An areal view of the 1 km^2 array area is shown in Fig. 1.

The following seven experiments were performed with the arrays described in the reports of the Air Shower Division.

Giant Air Shower (GAS)

- a) Observation of ultra-high-energy cosmic rays (M. Teshima, ICRR)
- b) Prototype detector for Telescope Array (M. Sasaki, ICRR)

Fig. 1. Aerial view of the Akeno 1 km^2 array area.

C: Central laboratory	D: Dormitory
S: Sub-electronics stations	M: Muon detectors (1 GeV)
ME: Muon detectors (0.5 GeV)	Cal: Calorimeter

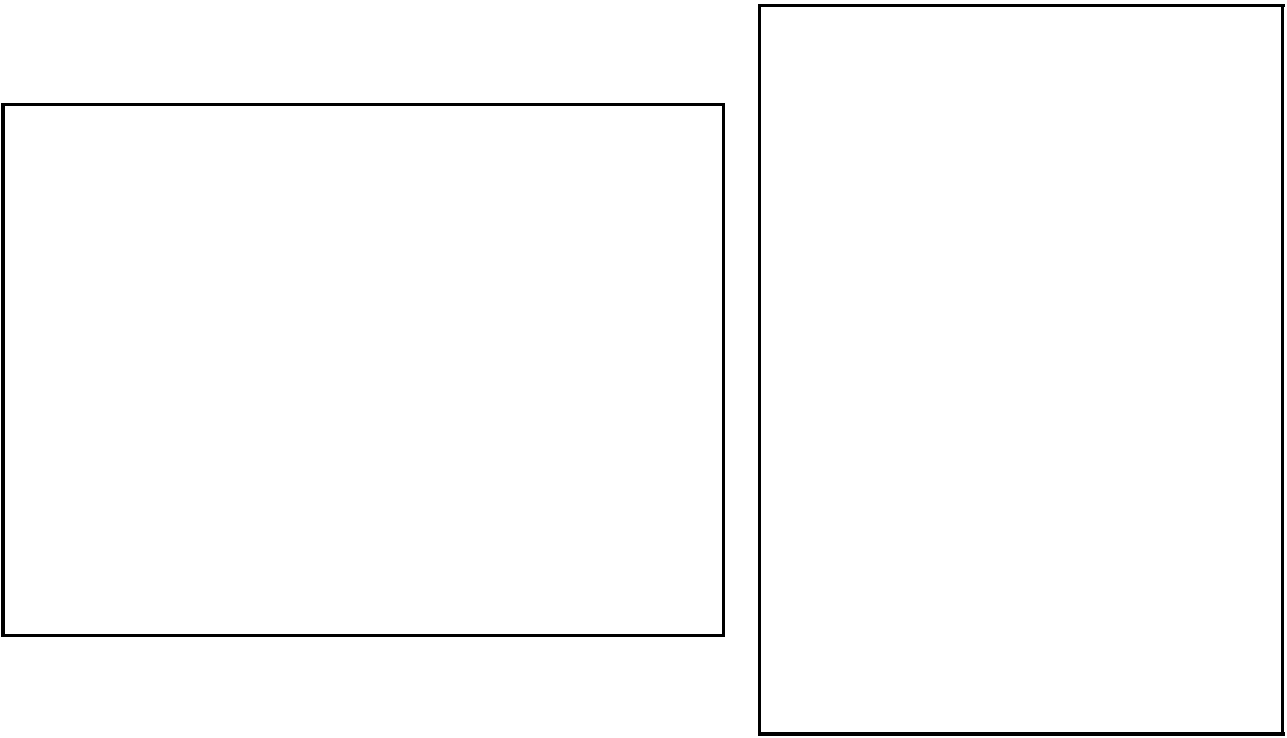
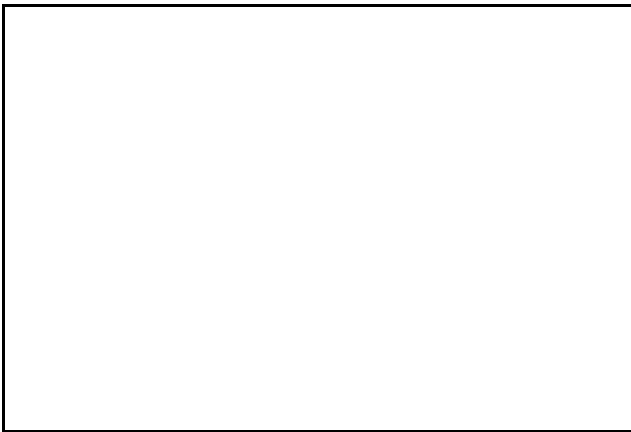


Fig. 2. One of the detector stations of Akeno Giant Air Shower Array (AGASA) ((a) outside, (b) inside)



- c) Arrival-time distribution of electrons of GAS at far from the core (K. Honda, Yamanashi Univ.)
- d) The observation of electron and muon components with lead-burger detector (S. Kawakami, Osaka City Univ.)
- e) Prototype detector for Pierre Auger project (J. W. Cronin, Univ. of Chicago)
- f) Study of EAS above 10^{16} eV (H. Sakuyama, Meisei Univ.)
- g) Preliminary study of detemination of chemical composition of cosmic rays above *knee* region (F. Kakimoto, Tokyo Tech.)

Fig. 3. View of a prototype water Čerenkov detector and a tent for a 3 m dish telescope.

Appendices

A. ICRR International Workshop

B. Seminar in 2001

C. List of Publications

- (a) Papers Published in Journals
- (b) Conference Papers
- (c) ICCR-Report

D. Doctoral Theses

E. Public Relations

ICCR News

F. List of Committee Members

- (a) Board of Councillors
- (b) Executive Committee
- (c) Advisory Committee

G. List of Personnel

A. ICRR International Workshop

The 2nd TAMA symposium
 Date 2002/02/06–08
 Sanjo Kaikan (7-3-1, Hongo, Bunkyo, Tokyo, Japan)
 (Cooperate with Tokyo university)

International Workshop on Technique and Application of Xenon Detectors

On December 3 and 4, 2001, we will have a two-day workshop concentrated on experiments using Xenon. The workshop will be held at Kashiwa-campus of the Institute for Cosmic Ray Research, Univ. of Tokyo, Japan. The purpose of this workshop is to discuss all aspects of experiments using Xenon, including problems and techniques.

One of the rare gases, Xenon, is very promising material of detectors for particle and astrophysics. This is owing to special properties of Xenon: (1) large scintillation output, (2) large atomic number, (3) fast timing response, (4) long life for ionized electrons, (5) particle identification power, (6) large density of liquid, (7) no long-life radio isotope, and so on. Those prominent properties makes many physicist interested in detectors using Xenon. Recently, we have many kinds of future plans for large-scale Xenon detectors around the world. In particular, some of them will use several tons of Xenon. Although their goals are different, we are frequently required to solve same kinds of problem. Because of such situation, we feel that it is a reasonable time to organize an international technical workshop concentrated on this subject. We hope our workshop exhaustively covers all applications using Xenon.

Purpose of the Workshop Xenon is used and planning for gamma ray detectors, double beta decay experiments, dark matter search experiments, solar neutrino experiments, and so on. The purpose of this technical workshop is to form a new strong community in which information and techniques of Xenon are intensively studied and shared, and to exchange our knowledge and status of planning detectors. The subjects which will be covered are: 1) various detector technologies, 2) purification of Xenon, 3) PMT development, 4) Xenon production, 5) enrichment, 6) calibration, 7) low background environment, 8) applications for various physics, etc.

This workshop is supported by the Grants-in-Aid for Scientific Research on Priority Areas A, “Neutrino Oscillations and Their Origin,” from the Ministry of Education, Culture, Sports, Science, and Technology, Japan.

Participants

41 from Japan, 8 from USA, 3 from Germany, 2 from Italy, 2 from UK, 1 from Ruccia, 1 from Ukraine, 1 from Portugal

The 3rd Workshop on “Neutrino Oscillations and Their Origin”

The 3rd International Workshop on Neutrino Oscillations and their Origin (NOON2001) will be held at Kashiwa-campus of the Institute for Cosmic Ray Research, University of Tokyo, Japan, December 5th through December 8th of 2001.

Initiated by the discovery of neutrino oscillations in atmospheric neutrinos in Super-Kamiokande, the series of the workshop entitled “Neutrino Oscillations and their Origin” has been held since 2000 in Japan. In this year, another evidence for neutrino oscillations has been found in solar neutrinos, combining the results of Super-Kamiokande and SNO results. These discoveries carry the investigation of neutrino oscillations a step further and give us hints to search for the origin of neutrino masses. In the workshop, we will discuss latest experimental results, phenomenological theoretical analysis, and theoretical implications which predicts neutrino oscillations. Topics in the workshop are atmospheric neutrinos (experimental results and flux predictions), solar neutrinos (experimental results, solar models and nuclear cross sections), phenomenology of the neutrino oscillations, theoretical origin of neutrino oscillations (GUTs etc.), and lepton flavor violation processes. As a 3rd workshop, we have a stress on the following subjects:

1) precisions of the determination of the mixing and mass matrices in near future; 2) theoretical implications of the different solar neutrino solutions, MSW-LMA, LOW or quasi-Vacuum; 3) constraints on the sterile neutrinos from the experimental data; 4) constraint on neutrino masses from supernovae, 5) relation between neutrino oscillations and double beta decay, and so on.

In this workshop, we bring experimentalists and theorists together and discuss about those subjects.

This workshop is supported by the Grants-in-Aid for Scientific Research on Priority Areas A, "Neutrino Oscillations and Their Origin," from the Ministry of Education, Culture, Sports, Science, and Technology, Japan.

Participants

68 from Japan, 9 from USA, 4 from Italy, 3 from Germany, 2 from Switzerland, 2 from UK, 1 from Ruccia, 1 from Ukraine, 1 from Portugal

B. Seminar in 2001

Date	Title	Lecturer
6 June 2001	Developments of Superstring theory and nonperturbative field theory	T. Eguchi
12 June 2001	Trajectory tracing in empirical geomagnetospheric models: Suggestion for plasma transport to the magnetotail	K. Seki
28 June 2001	Observational cosmology	N. Sugiyama
4 July 2001	BESS experiment	Y. Asaoka
5 July 2001	B physics from Lattice NRQCD	J. Shigemitsu
6 July 2001	Quantum Computing and Biophysics	A. D. Patel
16 July 2001	Domain Walls in Cosmology: Old Problems and New Solutions	Y. V. Dumin
26 July 2001	The Alpha Magnetic Spectrometer, an experiment to search for dark matter and antimatter on the ISS	R. Battiston
17 September 2001	Gamma ray emission from AGN and pulsars	Q. Luo
27 September 2001	Present Status of Auger Project in Argentine	R. Biral
28 September 2001	Measurement of the Charged Current ^8B Solar Neutrino Flux with the Sudbury Neutrino Observatory	F. Duncan
22 October 2001	How much can intervening magnetic fields affect our understanding of the nature of Ultra High Energy Cosmic Ray?	G. M. Tnaco
26 October 2001	The K2K Participation in the Harp Experiment	J. Hill
31 October 2001	The theory of physical combination	T. Miwa
27 November 2001	The Origin of the Hubble Sequence of Galaxy Types	R. Ellis
29 November 2001	The recent topics about ultra high energy air shower	M. Teshima
20 December 2001	Hard X-ray emission from the galactic disk and spectrum of subrelativistic cosmic rays	V. A. Dogiel
21 December 2001	New Results from K2K	J. Hill
24 January 2002	Cosmic Ray Propagation and the Cosmic Ray Source Spectrum	R. Clay
13 February 2002	The study of jet activity by multi-wavelength observation of Blazars	C. Tanihata
15 February 2002	Dark matter search by LiF bolometer in deep underground	K. Miuchi
18 February 2002	Horizontal Showers from Haverah Park and Auger observatory	R. Vazquez
4 March 2002	From Big Crunch to Big Bang	J. Maharana

18 March 2002	SciFi detector in K2K experiments and the current results	T. Iwashita
19 March 2002	Baksan Neutrino experiments: data and analysis	A. V. Butkevich

C. List of Publications — 2001 fiscal year

(a) Papers Published in Journals

1. “Effect of Multiple Scattering in the Lidar Measurement of Tropospheric Aerosol Extinction Profiles,” W. Widada, H. Kinjo, H. Kuze, N. Takeuchi and M. Sasaki, *OPTICAL REVIEW* Vol. 8, No. 5 382–387 (2001)
2. “The Optical Reflector System for the CANGAROO-II Imaging Atmospheric Cherenkov Telescope,” *Astropart. Phys.* **14** 261 (2001)
3. “Phenomenological approach of multiple particle production at high energies: Energy distribution of produced particles by data of direct observation,” *Physical Review* **D64** 054004 (2001)
4. “Cryogenic contamination speed of an ultra-low loss mirror for the cryogenic laser interferometer,” S. Miyoki et al., *Cryogenics* **41** 415 (2001).
5. “Cryogenic measurement of the optical absorption coefficient in sapphire crystals at 1.064 μm for the large-scale cryogenic gravitational wave telescope,” T. Tomaru et al., *Physics Letter A* **283**, 80 (2001)
6. “Stable operation of a 300-m laser interferometer with sufficient sensitivity to detect gravitational-wave events within our galaxy,” M. Ando, et al., *Phys. Rev. Lett.* **86**, 3950–3954 (2001).
7. “First search for gravitational waves from inspiraling compact binaries using TAMA300 data,” H. Tagoshi, et al., *Phys. Rev. D* **63**, 062001 (2001).
8. “ ^8B and hep Neutrino Measurements from 1258 Days of Super-Kamiokande Data,” The Super-Kamiokande Collaboration, *Phys. Rev. Lett.* **86**, 5651–5655 (2001)
9. “Constraints on Neutrino Oscillations Using 1258 Days of Super-Kamiokande Solar Neutrino Data,” The Super-Kamiokande Collaboration, *Phys. Rev. Lett.* **86**, 5656–5660 (2001)
10. “ ^{16}N as a calibration source for Super-Kamiokande,” The Super-Kamiokande Collaboration, *Nucl. Instr. & Meth. A* **458**, 636–647 (2001)
11. “Comparison of three-dimensional and one-dimensional schemes in the calculation of atmospheric neutrinos,” M. Honda et al., *Phys. Rev. D*, **64** (2001) 053011.
12. “Observation of atmospheric neutrinos,” T. Kajita and Y. Totsuka, *Rev. Mod. Phys.* **73** (2001) 85.
13. “Oscillations of atmospheric neutrinos,” C. K. Jung et al., *Ann. Rev. Nucl. Part. Sci.*, **51** (2001) 451.
14. “Method for determination of ^3He in neutrino oscillation appearance experiments,” T. Kajita, H. Minakata and H. Nunokawa, *Phys. Lett. B*, **528** (2002) 245.

(b) Conference Papers

1. “Energy estimation of AGASA events,” N. Sakaki for the AGASA Collaboration Proc. of 27th ICRC, Hamburg, 2001, Vol. 1, 329 (2001)
2. “Cosmic Ray Energy spectrum above 3×10^{18} eV,” N. Sakaki for the AGASA Collaboration Proc. of 27th ICRC, Hamburg, 2001, Vol. 1, 333 (2001)
3. “Anisotropy of cosmic-ray arrival direction at 10^{18} eV observed by AGASA,” M. Teshima for the AGASA Collaboration Proc. of 27th ICRC, Hamburg, 2001, Vol. 1, 337 (2001)
4. “Clusters of Cosmic Rays above 10^{19} eV observed with AGASA,” M. Takeda for the AGASA Collaboration Proc. of 27th ICRC, Hamburg, 2001, Vol. 1, 341 (2001)

5. “Muon component in giant air showers with energies greater than $10^{18.5}$ eV observed by AGASA,” N. Inoue for the AGASA Collaboration Proc. of 27th ICRC, Hamburg, 2001, Vol. 1 345 (2001)
6. “Properties of EHE gamma-ray initiated air showers and their search by AGASA,” (89 kB) K. Shinozaki for the AGASA Collaboration Proc. of 27th ICRC, Hamburg, 2001, Vol. 1 346 (2001)
7. “A search for horizontal air showers induced by extremely high energy cosmic neutrinos observed by Akeno Giant Air Shower Array,” S. Yoshida for the AGASA Collaboration Proc. of 27th ICRC, Hamburg, Vol. 3 1142 (2001)
8. “Likelihood Analysis of sub-TeV Gamma-rays from RXJ1713-39 with CANGAROO-II,” R. Enomoto et al. Proc. of 27th ICRC, Hamburg, 2001, Vol. 5, 2477–2480 (2001)
9. “Observation of TeV Gamma-rays from NE-rim of SN1006 with CANGAROO-II 10 m Telescope,” S. Hara et al. Proc. of 27th ICRC, Hamburg, 2001, Vol. 5, 2455–58 (2001)
10. “Development of Light Guides for the Camera of CANGAROO-III Telescope,”— F. Kajino et al. Proc. of 27th ICRC, Hamburg, 2001, Vol. 5, p. 2909 (2001)
11. “Data Acquisition System of the CANGAROO-III Telescope,” H. Kubo et al. Proc. of 27th ICRC, Hamburg, 2001, Vol. 5, pp. 2900–2903 (2001)
12. “Observations of PSR1706-44 with CANGAROO-II Telescope,” J. Kushida et al. Proc. of 27th ICRC, Hamburg, 2001, Vol. 6, 2424–2427 (2001)
13. “The CANGAROO-III Project: Status Report,”—M. Mori et al. Proc. of 27th ICRC, Hamburg, 2001, Vol. 5, 2831–2834 (2001)
14. “Very High Energy Gamma-ray Observation of Southern AGNs with CANGAROO-II Telescope,” K. Nishijima et al. Proc. of 27th ICRC, Hamburg, 2001, Vol. 5, 2626–2629 (2001)
15. “Search for Gamma-rays above 10 TeV from Markarian 421 in a High State with the CANGAROO-II Telescope,” K. Okumura et al. Proc. of 27th ICRC, Hamburg, 2001, Vol. 5, 2679–2682 (2001)
16. “Study of the TeV Gamma-ray Spectrum of SN 1006 around the NE Rim,” T. Tanimori et al. Proc. of 27th ICRC, Hamburg, 2001, Vol. 6, 2465–2468 (2001)
17. “Multi-TeV gamma-ray emission from the Crab Nebula observed with the new Tibet-III air shower array,” M. Amenomori et al., Proc. of 27th ICRC, Hamburg, 2001, Vol. 6, 2395–2398 (2001).
18. “Multi-TeV gamma-ray observation of several strong outbursts of Mrk421 during 2000 and 2001 with the Tibet-III air-shower array,” M. Amenomori, et al., Proc. of 27th ICRC, Hamburg, 2001, Vol. 6, 2661–2664 (2001).
19. “Performance of the Tibet-III air-shower array,” M. Amenomori et al., Proc. of 27th ICRC, Hamburg, 2001, Vol. 2, 572–576 (2001).
20. “Search for TeV burst-like events coincident with the BATSE bursts using the Tibet air shower array,” M. Amenomori et al., Proc. of 27th ICRC, Hamburg, 2001, Vol. 7, 2753–2756 (2001)
21. “Primary proton flux around the “knee” region deduced from the observation of airshowers accompanied by gamma-ray families,” M. Amenomori et al., Proc. of 27th ICRC, Hamburg, 2001, Vol. 1, 18–21 (2001)
22. “Upper limit of diffuse gamma rays from galactic plane using the data with Tibet and HD array,” M. Amenomori et al., Proc. of 27th ICRC, Hamburg, 2001, Vol. 6, 2344–2347 (2001)
23. “Sun’s shadow in a high state of solar activity detected with the Tibet air shower array,” M. Amenomori et al., Proc. of 27th ICRC, Hamburg, 2001, Vol. 1, 18–21 (2001)
24. “A wide sky survey to search for TeV gamma-ray sources by the Tibet air shower array,” M. Amenomori et al., Proc. of 27th ICRC, Hamburg, 2001, Vol. 6, 2544–2547 (2001)
25. “The flux and spectrum of solar neutrinos at Super-Kamiokande,” E. Blaufuss for the Super-Kamiokande Collaboration, Proc. of 27th ICRC, Hamburg, 2001, Vol. 7, 3005 (2001)
26. “Recent results from Super-Kamiokande on atmospheric neutrinos,” J. Kameda for the Super-Kamiokande Collaboration, Proc. of 27th ICRC, Hamburg, 2001, Vol. 3, 1057 (2001)

27. "A search for astronomical neutrino sources with the Super-Kamiokande detector," S. Matsuno for the Super-Kamiokande Collaboration, Proc. of 27th ICRC, Hamburg, 2001, Vol. 3, 1065 (2001)
28. "Discriminating between $\nu_\mu\nu_\tau$ and $\nu_\mu\nu_{sterile}$ in atmospheric ν_μ oscillations with the Super-Kamiokande detector," A. Habis for the Super-Kamiokande Collaboration, Proc. of 27th ICRC, Hamburg, 2001, Vol. 3, 1061 (2001)
29. "Search for nucleon decay in Super-Kamiokande," K. Kobayashi for the Super-Kamiokande Collaboration, Proc. of 27th ICRC, Hamburg, 2001, Vol. 4, 1459 (2001)
30. "Very High Energy Gamma Rays from Active Galactic Nuclei," T. Kifune, Proc. of AGN Variability Across the Electromagnetic Spectrum Sydney, Australia, (June 25–29, 2001), Publ. Astron. Soc. Australia, Vol. 19, No. 1 1–4 (2002)
31. "Very High Energy Gamma-Ray Observations of AGNs with CANGAROO," K. Nishijima, Proc. of AGN Variability Across the Electromagnetic Spectrum Sydney, Australia, (June 25–29, 2001), Publ. Astron. Soc. Australia, Vol. 19, No. 1 26–28 (2002)
32. "CANGAROO-II and CANGAROO-III," M. Mori, Proc. of Gamma-Ray Astrophysics 2001 Baltimore, USA (April 4–6, 2001), AIP Conference Proceedings 587, 927–931
33. "The Telescope Array Project," M. Sasaki et al., Proceeding of EHECR 2001, International Workshop on Extremely High Energy Cosmic Rays

(c) ICRR-Report

1. ICRR-Report-473-2001-3
"Doctor Thesis: Lepton T-and CP-violation search with neutrino factory"
Masafumi Koike
2. ICRR-Report-476-2001-6
"Muon anomalous magnetic moment, lepton flavor violation, and flavor changing neutral current processes in SUSY GUT with right handed neutrino"
Seungwon Baek, Toru Goto, Yasuhiro Okada, and Ken-ichi Okumura
3. ICRR-Report-478-2001-8
"Contributions to the 27th International Cosmic Ray Conference, Hamburg, Germany, August 7–15, 2001"
CANGAROO collaboration
4. ICRR-Report-479-2001-9
"Study of high energy cosmic ray interactions and primary composition at energies 10^{15} – 10^{17} eV using mountain based detectors"
V. Kopenkin, Y. Fujimoto, A. Ohsawa, C. E. Navia, C. R. A. Augusto and H. Semba
5. ICRR-Report-480-2001-10
"Contributions to 27th International Cosmic Ray Conference (07–15 Aug. 2001, Hamburg) from Cosmic Ray Collaboration at Mt. Chacaltaya"
A. Ohsawa
6. ICRR-Report-481-2001-11
"The Telescope Array Project: To appear in the Proceedings of the EHECR2001, International Workshop on Extremely High Energy Cosmic Rays (ICRR Kashiwa, Japan, 22–23 March 2001)"
Makoto Sasaki
7. ICRR-Report-482-2001-12
"Dissertation: Constraints of the neutrino oscillation parameters from 1117 day observation of solar neutrino day and night spectra in Super-Kamiokande"
Nobuyuki Sakurai

D. Doctor Thesis

S. Hara

Title: *Observation of TeV Gamma-Rays from the Supernova Remnant SN1006 with CANGAROO-II Telescope*
 Course: Doctor (Tokyo Institute of Technology)

S. Nagano

Title: *A Study of Frequency and Intensity Stabilization System with a High-power Laser for the TAMA300 Gravitational-wave Detector*
 Course: Doctor (University of Tokyo)

O. Miyakawa

Title: *Development of a Variable-Bandwidth Laser Interferometer Gravitational Wave Detector*
 Course: Doctor (University of Tokyo)

Andrew L. Stachyra

Title: *A Search for Astrophysical Point Sources of Neutrinos with Super-Kamiokande*
 Course: Doctor (University of Washington)

E. Public Relations

ICRR News

ICRR News is a newspaper published quarterly in Japanese to inform the Institute's activities. This year's editors were M. Sasaki and M. Ohnishi. It includes :

1. reports on investigations by the staff of the Institute or made at the facilities of the Institute,
2. reports of international conferences on topics relevant to the Institute's research activities,
3. topics discussed at the Institute Committees,
4. list of publications published by the Institute [ICRR-Report, ICRR-Houkoku(in Japanese)],
5. list of seminars held at the Institute,
6. announcements,
7. and other items of relevance.

The main topics in the issues in 2001 fiscal year were :

No. 45 (May 31, 2001)

- The statement from the old and new director (M. Yoshimura and Y. Totsuka)

No. 46 (August 31, 2001)

- The current status of CANGAROO (M. Mori)
- TAMA300 and LCGT (K. Kuroda)
- The report of Kashiwa clerk office (I. Hada)

No. 47 (December 31, 2001)

- Report of Super-Kamiokande accident (M. Yoshimura)
- Origin of the baryon number in universe, dark matter and Q ball (M. Kawasaki)
- Report of 27th international cosmic ray conference (T. Kajita, K. Okumura, M. Takita, M. Fukushima)
- Report of the inspection of the Minister of Education, Science and Culture in Super-Kamiokande (Y. Suzuki)
- Report of the open house in ICRR (M. Takita)

F. List of Committee Members

(a) Board of Councillors

YOSIMURA, Motohiko	ICRR, University of Tokyo
SUZUKI, Yoichiro	ICRR, University of Tokyo
KURODA, Kazuaki	ICRR, University of Tokyo
FUKUSHIMA, Masami	ICRR, University of Tokyo
SATO, Katsuhiko	University of Tokyo
KAJINO, Shinithi	University of Tokyo
YAMADA, Sakue	KEK
MASKAWA, Toshihide	Kyoto University
KAIFU, Norio	National Astronomical Observatory
SATO, Humitaka	Konan University
EJIRI, Hiroyasu	Osaka University
NAGASHIMA, Yorikiyo	Osaka University
OHTA, Itaru	Utsunomiya University
NISHIDA, Tokuhiko	Japan Society for the Promotion of Science
ITO, Nobuo	Osaka City University

(b) Executive Committee

YOSHIMURA, Motohiko	ICRR, University of Tokyo
AIHARA, Hiroaki	University of Tokyo
KOYAMA, Katsuji	Kyoto University
NISHIKAWA, Koichiro	Kyoto University
MATSUOKA, Masaru	National Space Development Agency of Japan
OHTA, Itaru	Utsunomiya University
MURAKI, Yasushi	Nagoya University
SAKATA, Michinori	Konan University
YANAGIDA, Tsutomu	University of Tokyo
MOTOBAYASHI, Toru	Rikkyo University
KURODA, Kazuaki	ICRR, University of Tokyo
SUZUKI, Yoichiro	ICRR, University of Tokyo
FUKUSHIMA, Masami	ICRR, University of Tokyo
TAKITA, Masato	ICRR, University of Tokyo

(c) Advisory Committee

MURAKI, Yasushi	Nagoya University
TAKITA, Masato	ICRR, University of Tokyo
MATSUBARA, Yutaka	Nagoya University
YANAGITA, Shohei	Ibaraki University
KAJINO, Fumiyoshi	Konan University
NISHIJIMA, Kyoshi	Tokai University
TORII, Shoji	Kanagawa University
MUNAKATA, Kazuki	Sinshu University
MIZUTANI, Kohei	Saitama University
SAKURAI, Takahisa	Yamagata University

KANEYUKI, Kenji
 SASAKI, Makoto
 MORI, Masaki
 OHASHI, Masataka
 SEKIGUCHI, Masaki

ICRR, University of Tokyo
 ICRR, University of Tokyo
 ICRR, University of Tokyo
 ICRR, University of Tokyo
 ICRR, University of Tokyo

G. List of Personnel

Director	YOSHIMURA, Motohiko
Kamioka group	
Scientific Staff	TOTSUKA, Yoji, SUZUKI, Yoichiro, NAKAHATA, Masayuki, ITOH, Yoshitaka, FUKUDA, Yoshiyuki, MIURA, Makoto, TAKEUCHI, Yasuo, SHIOZAWA, Masato, KOSHIO, Yusuke, MORIYAMA, Shigetaka, OBAYASHI, Yoshihisa
Chief Secretary	GOTO, Shohachiro
Technical Staff	YOKOKAWA, Keiji, FURUTA, Noboru
Research Fellows	NAMBA, Toshio, KAMEDA, Jun
Secretary	OHTSUBO, Junko, MORITA, Yasuko, TAJIKA, Sonoko
Research Center for Cosmic Neutrinos	
Scientific Staff	KAJITA, Takaaki, KANEYUKI, Kenji, OKADA, Atsushi
Technical Staff	SHINOHARA, Masanobu
Visiting Scientist	BUTKEVICH, A. V., HILL, James E.
Research Fellows	HONDA, Morihiro
Secretary	FUKUDA, Yoko
CANGAROO group	
Scientific Staff	ENOMOTO, Ryoji, MORI, Masaki, HATANO, Yoshikazu, KAWACHI, Akiko
Research Fellows	OKUMURA, Kimihiro, KSENOFONTOV, L.
TA/AGASA group	
Scientific Staff	FUKUSHIMA, Masami, TESHIMA, Masahiro, SASAKI, Makoto, HAYASHIDA, Naoaki
Technical Staff	TORII, Reiko, OHOKA, Hideyuki, SHIMODAIRA, Hideaki, AOKI, Toshifumi
Research Fellows	TAKEDA, Masahiro, YAMAMOTO, Tokonatsu WIENCKE, L., CHA, M., SAKURAI, Nobuyuki
Emulsion Division	
Scientific Staff	TAKITA, Masato, OHSAWA, Akinori, OHNISHI, Munehiro
Technical Staff	TOYODA, Setsuko, KOBAYASHI, Takahide
Research Fellows	KOPENKIN, Vladimir, Xu Xianwu, SHIOMI, Atsushi, TSUCHIYA, Harufumi, OUCHI, Tatsumi
Theory group	
Scientific Staff	YOSHIMURA, Motohiko, HISANO, Junji
Research Fellows	TAKEDA, Koujin, MATSUMOTO, Shigeki, YOKOI, Naoto, UESUGI, Tomoko
Mu Nu Division (Gravitational Wave group)	
Scientific Staff	KURODA, Kazuaki, OHASHI, Masataka, MIYOKI, Shinji
Technical Staff	ISHIZUKA, Hideki, YAMAMOTO, Kuniyuki
Research Fellows	TAYLOR, Colin T. YAMAMOTO, Kazuhiro
(SDSS group)	
Scientific Staff	FUKUGITA, Masataka, SEKIGUCHI, Masaki
Research Fellows	NAKAMURA, Osamu
Norikura	
Technical Staff	AGEMATSU, Yoshiaki, USHIMARU, Tsukasa

Post Graduate Students

KOBAYASHI, Kazuyosi (D3), NAKAYAMA, Shoei (D3),
YAMADA, Shuei (D3), OSONE, Satoko (D3),
IZU, Kouhei (D3), MIYAKAWA, Osamu (D3),
SUZUKI, Rieko (D2), KIMURA, Masahiko (D2),
ISHITSUKA, Masaki (D1), KATAGIRI, Hideaki (D1),
TSUCHIYA, Ken-ichi (D1), MASE, Keiichi (D1),
MANAGO, Naohiro (D1), OKUTOMI, Akira (D1),
KASAHARA, Kunihiko (D1), GOTO, Tomotsugu (D1),
INADA, Naohisa (D1), OHISHI, Michiko (M2),
KABUKI, Shigeto (M2), TSUNOO, Hajime (M2),
TSUJIKAWA, Yoshihiro (M2), JOBASHI, Masashi (M2),
MASUDA, Masataka (M2), HAYASHI, Maoto (M2),
TSUJI, Isao (M2), KONDO, Kazuhiro (M2),
TOKUNARI, Masao (M2), OYABU, Takato (M1),
UCHIDA, Tadashi (M1), KURASAWA, Katsumi (M1)

Administration Division
Staff

HADA, Isao, IGARASHI, Tsutomu, NAKAMURA, Hiroshi,
FURUKAWA, Toshiko, SHIZUKAI, Saori,
WATANABE, Hiroko, TASHIRO, Megumi, KOKUBUN, Yayoi,
IINUMA, Yuri, ASANO, Kouji, HIRUKAWA, Seiji,
MARUMORI, Yasuko, AKIYAMA Makiko, TANAKA, Sae,
MOTOIKE, Wakana, TAKAHASHI, Akiko

Technical Staff

KOBAYASHI, Masanobu